

DETERMINATION OF DYNORPHINS AND TNF- α BY LC-MS/MS IN
BIOLOGICAL SAMPLES: APPLICABLE TO STUDYING INFLAMMATORY
MECHANISMS

KARTHIK CHANDU

Bachelor of Pharmacy

Osmania University

June 2010

Master of Pharmacy

Jawaharlal Nehru Technological University

May 2013

submitted in partial fulfillment of requirements for the degree

DOCTOR OF PHILOSOPHY IN CLINICAL AND BIOANALYTICAL CHEMISTRY

At

CLEVELAND STATE UNIVERSITY

August 2020

©COPYRIGHT BY KARTHIK CHANDU 2020

We hereby approve this doctoral dissertation for

KARTHIK CHANDU

Candidate for Doctor of Philosophy in Clinical-Bioanalytical Chemistry for the

Department of Chemistry

and

CLEVELAND STATE UNIVERSITY

College of Graduate Studies by

_____ Date: _____

David Anderson, Ph.D., Dissertation Chairperson
Department of Chemistry, Cleveland State University

_____ Date: _____

Aimin Zhou, Ph.D., Committee member;
Department of Chemistry, Cleveland State University

_____ Date: _____

Bin Su, Ph.D., Committee member
Department of Chemistry, Cleveland State University

_____ Date: _____

Tony. L. Sahley, Ph.D., Committee member
School of Health Sciences & BGES , Cleveland State University

_____ Date: _____

Yana Sandler, Ph.D., Committee member
Department of Chemistry, Cleveland State University

June 1, 2020

Student's Date of Defense

DEDICATION

This work is dedicated to my parents Satyanarayana Chandu, Narmada Chandu and my wife Sreenivasavi Rayaprolu who worked selflessly behind the scenes by being my emotional support all through the years. It is their love, encouragement and support that propelled me forward every single time I slowed down and made my success journey enjoyable and memorable.

ACKNOWLEDGEMENTS

This work would not have been possible without the guidance of my committee chair, Dr. David J. Anderson for his wonderful support to make this possible, as an advisor, as well as a good friend.

I would like to extend my special thanks to Dr. Miyagi for taking his time out to teach me the proper way to learn the concepts of mass spectrometry and its application and for his recommendation and supplying the Lys-N proteolytic enzyme crucial to the success of this project.

I would like to specially thanks Dr. Sahley for always encouraging me and giving me the opportunity to work on the analytical part of the project and for always being available to help me understand the biological background of the experiment.

Thanks to Dr. Aimin Zhou, Dr. Bin Su for all their valuable suggestions during committee meetings and for their outstanding support and encouragement.

I would also like to thank my group members Sreenivasavi Rayaprolu, Eric Kipruto and Mst.Ummul Khair for all their timely support.

Special thanks to senior graduate student outside our group Dr. Shashank Gorityala and Dr. Chandana Mannem for sharing their experiences and expertise when I needed it.

Thanks to all other graduate students both within and outside Dr. Anderson's group that made this journey complete.

DETERMINATION OF DYNORPHINS AND TNF- α BY LC-MS/MS IN
BIOLOGICAL SAMPLES: APPLICABLE TO STUDYING INFLAMMATORY
MECHANISMS

KARTHIK CHANDU

ABSTRACT

Dynorphins are endogenous opioid peptides that have been implicated as initiators of immune and inflammatory response through upregulation of inflammatory cytokine and chemokine production, as well having a role in glutamate-induced neuro-inflammation and neurotoxicity. Being extremely potent peptides, the physiologic concentrations of dynorphins are very low ranging from 0.16 pg/mL during the absence of a stimulus to 23.5 pg/mL when stimulated in disease condition. Previously published HPLC-mass spectrometry techniques have insufficient detection capabilities for quantification and detection of dynorphins. As a result, immunoassay quantification has been the most utilized technique for analysis of dynorphins in physiologic samples. Although being sensitive, immunoassays have some inherent drawbacks of being complex multi-step process taking a long time to complete, challenge with reproducibility due to the non-specific binding interactions and the requirement of high sample volume. My dissertation focused on developing a sensitive LC-MS/MS technique to overcome such challenges in the analysis. A sensitive and robust LC-MS/MS assay has been developed and validated in the present work which can quantify the dynorphins below their low physiologic concentrations in mouse serum. To achieve this level of sensitivity, the intact peptide was digested using a novel metalloendopeptidase called Lys-N. This digestion process produced fragments which are extremely sensitive to detection by mass spectrometer and very specific to

dynorphin B. Sensitivity achieved by this method is 800 times more than previously published HPLC-mass spectrometry techniques.

TABLE OF CONTENTS

	Page
ABSTRACT.....	vi
LIST OF TABLES.....	xii
LIST OF FIGURES	xv
CHAPTER	
I. INTRODUCTION	1
1. Background.....	1
1.1. Physiologic Effects of Dynorphins	2
1.2. Cytokine/chemokine release in response to dynorphins.....	3
1.2.1. Other effects.....	3
1.3. Dynorphins in physiologic samples.....	4
1.3.1. Degradation process.....	4
1.3.2. Physiological concentrations	5
1.4. Quantification techniques	6
1.4.1. Non-spectroscopic techniques	6
1.4.2. Mass spectrometry in the analysis of dynorphins.....	7
1.4.3. Current mass spectrometry technique to analyze dynorphins.....	7
II. OVERVIEW OF LC-MS TECHNIQUES FOR QUANTIFYING PROTEINS AND PEPTIDES	8
2.1. Introduction to Mass Spectrometry for Biomolecules.....	8
2.2. Types of protein analysis	11
2.3. Sensitivity considerations for using digesting enzymes	13
2.4. Types of enzymes used in peptide and protein digestion	13
2.5. Factors affecting the mass spectrometry signal intensity in peptide determination	16

2.5.1. Instrumentation	16
2.5.2. Sample preparation	17

III. QUANTIFICATION OF DYNORPHINS BY LC-MS : RESULTS AND

DISCUSSION

3.1. Analytical background	21
3.2. Experimental	22
3.2.1. Chemicals.....	22
3.2.2. Instrumentation	22
3.2.3. liquid chromatography	23
3.2.4. Tandem mass spectrometry.....	23
3.2.5. Preparation of stock and working standard and Lys N solutions	24
3.2.6. Preparation of serum calibrators and quality controls	24
3.2.7. Digestion of the extracted peptide	25
3.2.8. Method validation	26
3.2.8.1. Calibration.....	26
3.2.9. Precision, accuracy and absolute extraction recovery	26
3.2.10. Selectivity, matrix effect and LLOQ	27
3.2.11. Stability studies.....	27
3.3. Results.....	27
3.3.1. Results for intact dynorphins	27
3.3.1.1. Mass spectrum results for intact dynorphin A	28
3.3.1.2. Mass spectrum results for intact alpha -neoendorphin	31
3.3.1.3. LC-MS/MS results of intact dynorphin A and alpha-neoendorphin.....	33
3.3.1.4. LC-MS/MS conditions.....	35
3.3.1.5. Discussion of results of intact dynorphins	36

3.3.1.6. Addressing the limitations of intact dynorphin MS analysis.....	36
3.3.2. Results for LC-MS/MS of Lys-N digested dynorphins	39
3.3.2.1. Digestion results and chromatogram separation of dynorphins results	39
3.3.2.2. Dynorphin A results.....	42
3.3.2.2.1. Liquid chromatogram of dynorphin A ...	42
3.3.2.2.2. Mass spectrometric detection of dynorphin A	43
3.3.2.2.3. Method validation of dynorphin A	44
3.3.2.3. Dynorphin B results	51
3.3.2.3.1. Liquid chromatogram of dynorphin B ...	51
3.3.2.3.2. Mass spectrometric detection of dynorphin B	52
3.3.2.3.3. Method validation of dynorphin B.....	53
3.3.2.4. Alpha neoendorphin results	60
3.3.2.4.1. Liquid chromatogram of alpha-neoendorphin	60
3.3.2.4.2. Mass spectrometric detection of alpha-neoendorphin	61
3.3.2.4.3. Method validation of alpha-neoendorphin	62
IV. TUMOR NECROSIS FACTOR – ALPHA	70
4.1. Cytokines - introduction	70
4.1.1. Tumor necrosis factor – alpha (TNF- α)	71
4.2. LC-MS method development.....	72
4.2.1. Chemicals.....	72
4.2.2. Instrumentation	72

4.2.3. Liquid chromatography.....	72
4.2.4. Tandem mass spectrometry.....	73
4.2.5. Preparation of stock and working standard solutions	73
4.2.6. Preliminary in-silico experiments	74
4.2.7. Mass spectrometry analysis	79
4.3. Future Experiments.....	79
4.3.1. Sample Preparation	79
4.3.2. LC-MS optimization	80
V. FUTURE DIRECTIONS	81
REFERENCES	83

LIST OF TABLES

Table	Page
I. Dynorphin peptides and their amino acid sequence	2
II. Pros and cons of commonly used mass analyzers	10
III. Types and number of proteases.....	14
IV. List of few commonly used proteases along with their cleavage sites	15
V. Fractionation methods and dependent physical or chemical property	20
VI. Expected m/z of intact dynorphin A.....	28
VII. Theoretical m/z values for alpha neoendorphin	32
VIII. MRM pair for dynorphin A and alpha-neoendorphin.....	33
IX. LLOD and LLOQ of dynorphin A and alpha neoendorphin	34
X. Expected post digestion peptide fragments of dynorphin A, dynorphin B and alpha- neoendorphin.....	38
XI. Observed cleavage sites and generated peptides for dynorphin A	39
XII. Amino acid sequence, charge states and molecular weights of the digested peptide fragments.....	40
XIII. Six replicates of 0.125 pg/mL calibrator in 6 lots of mouse serum	45
XIV. Percent recovery and % variance in four concentrations in pooled mouse serum.....	47

XV.	Matrix factor (MF) in three concentrations from six different lots of mouse serum.....	48
XVI.	Intra-day accuracy and precision for four concentrations with three replicates on the same day(n=6).....	49
XVII.	Inter-day accuracy and precision for four concentrations on three different days (n=6)	49
XVIII.	Stability of of dynorphin A at 2 temperatures (-22 °C, 10°C).....	50
XIX.	Six replicates of 0.125 pg/mL calibrator in 6 lots of mouse serum.....	54
XX.	Selectivity and Lower limit of quantification	55
XXI.	Percent recovery and % variance in four concentrations from six different replicates of pooled mouse serum.....	56
XXII.	Matrix factor (MF) in three concentrations from six different lots of mouse serum.....	57
XXIII.	Intra-day accuracy and precision for four concentrations with three replicates on the same day(n=6)	58
XXIV.	Inter-day accuracy and precision for four concentrations with three replicates on three different days (n=6)	58
XXV.	Stability of dynorphin B at three temperatures (-22 °C, 10°C, -20°C)	59
XXVI.	Six replicates of 0.125 pg/mL calibrator in 6 lots of mouse serum.....	64
XXVII.	Percent recovery and % variance in four concentrations in pooled mouse serum.....	66

XXVIII.	Matrix factor (MF) in three concentrations from six different lots of mouse serum.....	67
XXIX.	Intra-day accuracy and precision for four concentrations with three replicates on the same day(n=6)	68
XXX.	Inter-day accuracy and precision for four concentrations on three different days (n=6)	68
XXXI.	Stability of alpha neoendorphin at 2 temperatures (-22 °C, 10°C).....	69
XXXII.	Theoretical or calculated molecular weights	76
XXXIII.	Molecular weight of fragments accounting for alkylation during sample preparation	76
XXXIV.	m/z of the Theoretical Fragments in positive mode.....	77
XXXV.	m/z of the Theoretical Fragments in negative mode	77

LIST OF FIGURES

Figure	Page
1. Fragmentation patterns from CID producing b ions and y ions.....	9
2. Type of analysis and form of protein analyzed.....	12
3. Full spectrum scan of intact dynorphin A showing the relative intensities of detected m/z at an infusion rate of 10 $\mu\text{L}/\text{minute}$ at 10 $\text{pg}/\mu\text{L}$ in 15% ACN was infused.....	29
4. MS/MS of 430.5 m/z of intact dynorphin A.....	30
5. MS/MS of 537.8 m/z of intact dynorphin A.....	30
6. MS/MS of 716.8 m/z of intact dynorphin A.....	31
7. MS/MS spectrum of 410.5 m/z of intact alpha-neoendorphin.....	32
8. MS/MS spectrum of 615.2 m/z of intact alpha-neoendorphin.....	32
9. LLOD of dynorphin A and alpha-neoendorphin	34
10. Co-elution of dynorphin A (mrm pair: 537.8 – 136; 10 $\text{pg}/\mu\text{L}$) and.....	35
11. Trypsin cleavage sites on dynorphin B.....	37
12. Lys-N cleavage sites on dynorphin B.....	38
14. Separation of the three peptides dynorphin A YGGFLRRIRP fragment (m/z 412 \rightarrow 136), dynorphin B YGGFLRRQF fragment (m/z 572.5 \rightarrow 136.1) and alpha-neoendorphin YGGFLR fragment (m/z 712 \rightarrow 278) on a Luna Omega Polar C18 100 A LC column (25 $\mu\text{g}/\text{mL}$; Injection volume: 20 μL)	41
15. Chromatogram showing the retention time of dynorphin A YGGFLRRIRP fragment (m/z 412 \rightarrow 136) on a Luna Omega Polar C18 100 A LC column (concentration: 2.5 $\mu\text{g}/\text{mL}$; Injection volume: 20 μL)	42
16. Infusion mass spectrum of the Lys-N digested fragments of intact dynorphin A.....	43

17.	MS/MS of the daughter ions of digested YGGFLRRIRP fragment of intact dynorphin A	43
18.	Calibration plot of intact dynorphin A as measured by the YGGFLRRIRP fragment (m/z 412 →136) in three trials (n=3)	44
19.	Chromatogram showing the retention time of dynorphin A YGGFLRRIRP fragment (m/z 412 →136) at the lowest calibrator concentration	45
20.	Chromatogram of the blank serum with MRM set for m/z 412 →136	46
21.	Chromatogram showing the retention time of dynorphin B YGGFLRRQF fragment (m/z 572.5 →136.1) at the lowest calibrator concentration on a Luna Omega Polar C18 100 A LC column (Injection volume: 20 µL).....	51
22.	Infusion mass spectra of dynorphin B showing m/z of Lys-N digested fragment YGGFLRRQF of dynorphin B on the top and the daughter ion of 572.5 on the bottom	52
23.	Calibration plot of intact dynorphin B as measured by the YGGFLRRQF fragment	53
24.	Chromatogram showing the retention time of Lys-N digested fragment dynorphin B YGGFLRRQF fragment (m/z 572.5 →136.1) at the lower limit of quantification	55
25.	Chromatogram showing the small interferant peak retention time of Lys-N digested fragment dynorphin B YGGFLRRQF fragment (m/z 572.5 →136.1 ..	55

26.	Chromatogram showing the retention time of Lys-N digested alpha-neoendorphin fragment YGGFLR (m/z 712 →278) at the highest calibrator concentration on a Luna Omega Polar C18 100 A LC column, Injection volume: 20 µL.....	60
27.	Infusion mass spectra of the Lys-N digested fragments of intact alpha-neoendorphin (YGGFLR: m/z 712).....	61
28.	MS/MS spectrum of the daughter ions of digested YGGFLR (m/z 712) fragment of intact alpha-neoendorphin.....	62
29.	Calibration plot of intact alpha-neoendorphin as measured by the YGGFLR (m/z 712 →278) in three trials (n=3).....	63
30.	Chromatogram showing the retention time of alpha neoendorphin digested fragment YGGFLR (m/z 712 →278) at the lower limit of quantification	64
31.	Chromatogram of the blank serum showing no interferent peak when analyzed for Lys-N digested fragment YGGFLR of intact alpha-neoendorphin analyzed for mrm of 712 →278.....	65
32.	In-silico digested protein showing cleavage sites and probability.....	75
33.	Deconvoluted chromatogram showing the peak for one of the digested peptides of TNF-α (pink colored peak).....	78

CHAPTER I

INTRODUCTION

1. Background

Dynorphins are classified as endogenous opioid peptides [1–3] which bind preferentially to the κ -opioid receptors [2] and are formed from the 26 KDa precursor protein prodynorphin [4,5]. Prodynorphin is found in gut, posterior pituitary, and brain [6–9]. Immunoreactivity experiments in a hamster showed its presence in the hippocampal formation, lateral septum, bed nucleus of the stria terminalis, medial preoptic area, medial and central amygdaloid nuclei, ventral pallidum, substantia nigra, and numerous hypothalamic nuclei [10]. All the bioactive peptides that are formed are the C-terminal extensions of [Leu]enkephalin peptide sequence [11,12].

The endoproteolytic processing of prodynorphin is carried out by two primary protease pathways. The two pathways are cathepsin L cysteine protease in secretory vesicles and proprotein convertase 2 (PC2) proteases. This proteolysis of prodynorphin releases dynorphin A, dynorphin B, α -neoendorphin, β -neoendorphin [4,5,12–14] and leuomorphin (dynorphin B 1-29) [2,15] with the amino acid sequence [16,17] of each given in Table 1. The seventeen amino acid peptide, DYN-A(1–17) is further digested by these

peptidases resulting in structurally related peptides such as DYN-A (1–13), DYN-A(1–8) and Leu-enkephalin [2,6,18,19]. More details concerning the degradation of dynorphins are given in Section 1.3.1. The fragment dynorphin A-(1–13) is crucial for its potency [20]. The first four amino acid residues in the structure constitute the message region, and the amino acids from 5–13 are responsible for the potency and specificity for the κ -opioid receptors [21].

Table I: Dynorphin peptides and their amino acid sequence

Peptide	Sequence
Dynorphin A	YGGFLRRIRPKLKWDNQ
Dynorphin B	YGGFLRRQFKVVT
α -neoendorphin	YGGFLRKYPK
β -neoendorphin	YGGFLRKYP
Leumorphin	YGGFLRRQFKVVTRSQEDPNAYSGELFDA

1.1. Physiologic effects of dynorphins

Dynorphins play a regulatory role in numerous functional pathways. They play a significant role in the regulation of the immune/inflammatory system and are known to activate immune system functions that are associated with innate immunity [22,23]. Dynorphins are ligands for κ -opioid receptors and the expression of these receptors is very well regulated in the immune system [24–29]. In addition, they can influence the upregulation and release of monocytes/macrophages [30–32], polymorphonuclear leukocytes [33], and as well as proinflammatory cytokines [34–36]. Dynorphins also act

by the stimulating the production of oxygen free radicles [33], cause neuronal cell death by excitotoxic mechanisms altering glutamate levels, increase ion (K^+ , Ca^{+2} and Mg^{+2}) permeability of ion channels [37–41] and activate NMDA receptors [37,42–44].

1.2. Cytokine/chemokine release in response to dynorphins

Activation of NMDA receptors triggers a series of inflammatory interactions beginning with the activation of NF-kB [36,45,46], followed by an upregulation in the expression of proinflammatory cytokines such as TNF- α and IL-6 [32,47], which causes an upregulation in the expression of chemokines such as MCP-1/CCL2 [47–49] and proliferation of phagocytic leukocytes and lymphocytes [47,50]. Since dynorphins have the ability to affect the activation of the NMDA receptors, they are capable of starting the complete process of inflammatory interactions that lead to an increase in the production of proinflammatory cytokines, chemokines, and superoxides [32,51,52].

1.2.1. Other effects

Dynorphins are endogenous neuroactive opioid peptides that are known to play a role in a variety of physiological processes such as the regulation of pain [53–57], temperature [58], motor activity [59,60], the cardiovascular system [61,62], respiration, feeding behavior [63,64], hormonal balance, and responses to shock and stress [65]. The “non-opioid” effects of dynorphins also include neurological dysfunction, cytotoxicity, secondary tissue damage, paralysis, neural inflammation, and a potentiation of NMDA receptor sensitivity to glutamate leading to neuropathic hypersensitivity that is often associated with chronic peripheral tissue inflammation [37,42,57,59].

Dynorphins also act by stimulating the production of oxygen-based free radicals [33], causing neuronal cell death by excitotoxic mechanisms that include alterations in

glutamate levels, and increases in ion (K^+ , Ca^{+2} and Na^+) conductance's [37,66] by way of interactions at NMDA receptors [37,42,44]. A comprehensive review has been published [67].

1.3. Dynorphins in physiologic samples

1.3.1. Degradation process

As previously mentioned, the proteolysis of the precursor molecule prodynorphin releases dynorphin A, dynorphin B, α -neoendorphin, β -neoendorphin and leumorphin (dynorphin B 1-29)[2,15]. Among the dynorphins, dynorphin-B, as well as dynorphin-A (1-17) are relatively less susceptible to proteases [68] in normal physiological conditions. There are multiple kinds of peptidases that metabolize the dynorphin peptides. A few of the major peptidases involved are aminopeptidases [69], angiotensin-converting enzyme (ACE), insulin degrading enzyme [70], serine peptidases [71], dipeptidyl peptidase III and IV (DPP III, DPP IV) [72], which act to either convert a parent peptide sequence into an active form or to inactivate a physiologically active peptide [73,74].

Dynorphin A (1-17) has been shown to undergo very slow biotransformation and the products formed depend on the site at which it is released. It has been shown that rat brain, human and rhesus monkey blood show common product peptides after its metabolism [75]. During the initial 30 minutes, dynorphin A metabolized to dynorphin A (2-17), dynorphin A (3-17), dynorphin A (4-17), dynorphin A (5-17), dynorphin A (1-6), dynorphin A (7-17), dynorphin A (8-17), and dynorphin A (9-17). After a prolonged incubation time of 1 to 4 hours, it metabolized to dynorphin A (3-17), dynorphin A (4-17), and dynorphin A (5-17) [76–78].

Dynorphin A (1-13) has a very fast biotransformation rate, with the initial sequence metabolizing in 0.5-1 minute. A 30 min incubation period produced products such as dynorphin A (1-12), dynorphin A (4-12), dynorphin A (3-12), dynorphin A (2-12), dynorphin A (1-6), dynorphin A (5-11), and dynorphin A (5-12) [73,78].

1.3.2. Physiological concentrations

Being extremely potent, dynorphins are present in a very low concentrations in normal physiologic samples. Its concentration increases only in response to certain physiological stimuli. The concentrations of dynorphins varies with the type, location of the peptides and condition of the body (normal or stressed). The concentration of dynorphin-B in human serum can range from 0.16 pg/mL during the absence of a physiological stimulus to 23.5 pg/mL when stimulated by disease processes [32,33,79]. As these are very potent peptides, the increase in the physiological concentration when provoked, is relatively still low.

The concentrations of different dynorphins vary in different locations in the body. DYN-A(1–13) is capable of stimulating the production of cytokines such as TNF- α and IL-6 at a concentration of 0.16 pg/mL [32] and mediates the chemotaxis of macrophages at concentrations as low as 0.16 pg/mL, with peak effects observed at concentrations of 16.0 pg/mL to 16.0 ng/mL [31]. A concentration of 25.0 pmol/g was found in the substantia nigra and hypothalamus, whereas the other parts of the human post-mortem brain such as amygdala, hippocampus, periaqueductal grey, colliculi, pons, medulla and area postrema showed a relatively lower concentration [2].

1.4. Quantification techniques

1.4.1. Non-spectroscopic techniques

Immunoassay quantitation is the most utilized technique for determination of dynorphins at physiologic concentrations [34]. Immunoassays have been used extensively to analyze dynorphins for many years. Immunoassays use an antibody coated surface (usually a microplate or a microsphere) which is specific to the dynorphin of interest to capture the peptide and then another antibody specific to another site on the peptide called a reporter molecule is used to quantify the peptide present by comparing to a reference standard curve.

Though immunoassays have been used in the past, they have a few drawbacks [80] such as:

1. It is a complex multi-step process based on a biological reaction between an antibody and an antigen. Such reactions have an inherent issue of a lack of reproducibility due to non-specific binding, lot to lot variability in the antibody plates/microspheres used. These drawbacks lead to false positive and inconsistent results.
2. As the process involves multiple steps, the analysis takes a very long time to complete.
3. Due to the use of specific antibodies, it is not possible to differentiate and analyze multiple species of dynorphins at the same time.

Having such drawbacks warrants the requirement for a method which can not only overcome the challenges but also enhance the effectiveness and quality of analysis.

1.4.2. Mass spectrometry in the analysis of dynorphins

LC-MS as a tool for the analysis of dynorphins. LC-MS has an advantage when compared to immunoassays [80–82] due the fact that they are

1. Very robust and highly reproducible.
2. Extremely sensitive and precise
3. Requires very little sample for analysis
4. The process is majorly automated, thus reduces the possibility of human errors and can analyze multiple samples in a short period of time.
5. Multiple analytes can be differentiated and quantified at the same time

Being automated, LC-MS when coupled with informatic tools, has the capability to run and analyze multiple samples in minutes.

1.4.3. Current mass spectrometry technique to analyze dynorphins

Although in the past, LC-MS/MS, MALDI-IMS (imaging mass spectroscopy) and MALDI-TOF methods were developed and afforded the advantage of providing the simultaneous determination of individual dynorphins [83–87], none of these methods were established to quantify the very low physiological concentrations of dynorphins. The current project is focused on the development of a very sensitive LC-MS/MS method for the separation and quantification of all the dynorphins, α -neoendorphin and cytokines.

CHAPTER II

OVERVIEW OF LC-MS TECHNIQUES FOR QUANTIFYING PROTEINS AND PEPTIDES

2.1. Introduction to mass spectrometry for biomolecules

A mass spectrometer has three major components: an ion source (ionization of the analytes), mass analyzer (filters the ions based on mass-to-charge ratio) and a detector (produces signal that can be recorded). There are many different types of mass analyzers such as quadrupole, ion trap, time of flight and Fourier transform (ion cyclotron and orbitrap), and orbitrap. The choice of mass analyzer depends on the mass of the analyte, required resolving power, compatibility with desired ion source and desired limit of detection. The pros and cons of a few commonly used different mass analyzers are shown in Table II.

Mass spectrometry-based proteomics has an important technique for the qualitative and quantitative analysis of proteins and peptides in the field of bio-analysis.

Over the past decade, the technique has been developed with a major focus on the technological aspects of mass spectrometers to allow the quantification of proteins and peptides with the required accuracy, selectivity, and sensitivity [88]. This technique is now

being utilized at almost every stage of bio-molecule analysis starting from formulation development, stability studies, structural characterization (amino acid sequence, molecular weight, post-translational modifications and modification sites) and quality control.

Due to their large molecular weights, biomolecules such as proteins and peptides usually require high mass range and high-resolution instruments with MS/MS capabilities such as a quadrupole time-of-flight (Q-ToF) instrument or a more advanced hybrid orbitrap MS system. MS/MS is a process in the mass spectrometry which is used to obtain structural information for the proteins and peptides of interest. A wide range of fragmentation techniques such as collision-induced dissociation (CID), higher-energy collision dissociation (HCD), electron capture dissociation (ECD) and electron transfer dissociation (ETD) are used for MS/MS experiments. Collision-induced dissociation (CID) is the most used technique, with the fragmentation pattern of peptide bonds in proteins and peptides shown in Figure 1.

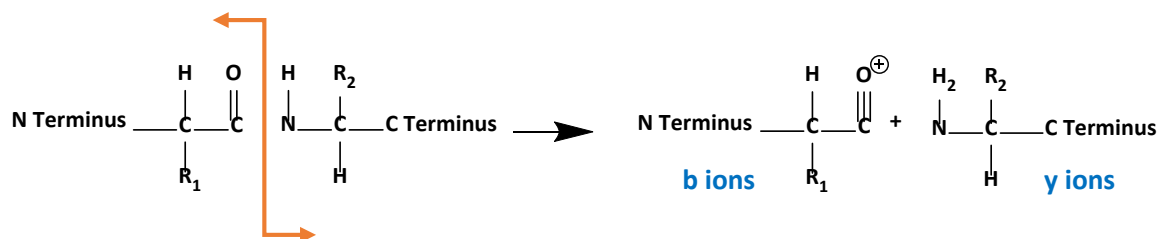


Figure 1: Fragmentation patterns from CID producing b ions and y ions

Table II: Pros and cons of commonly used mass analyzers [89–93]

S.No.	Mass analyzer	Pros and cons
1	Quadrupole	<p>Pros :</p> <ul style="list-style-type: none"> • Rugged, Reliable, and Sensitive • Less maintenance • Very rapid scan rate <p>Cons :</p> <ul style="list-style-type: none"> • Small mass range (not very suitable for large protein analysis) • Low resolution
2	Time of flight	<p>Pros:</p> <ul style="list-style-type: none"> • Highest mass range (Ideal for intact protein analysis) • Very fast scan speed • Excellent mass accuracy and high resolution • Improved dynamic range for quantification (newer instruments) • Capable of SWATH analysis (data-independent acquisition strategy that provides a very comprehensive quantitative analysis) <p>Cons:</p> <ul style="list-style-type: none"> • Difficulty of adaption to electrospray; High maintenance
3	Ion trap	<p>Pros :</p> <ul style="list-style-type: none"> • Simple design – Low cost; Small size; Well suited for tandem MS; Easy for positive/negative ions <p>Cons :</p> <ul style="list-style-type: none"> • Limited mass range – not as much a problem with current innovations • Medium resolution
5	Orbitrap	<p>Pros:</p> <ul style="list-style-type: none"> • High mass range (Ideal for intact protein analysis) • Fast scan speed • Excellent mass accuracy and high resolution • Capable of data-independent acquisition

Mass spectrometers are often coupled with a variety of chromatographic techniques. Chromatography techniques such as reversed phase and HILIC are compatible with mass spectrometry, whereas hydrophobic interaction (HIC), ion exchange (IEX), and size exclusion (SEC) chromatography are not directly compatible due to the use of salts that are not volatile.

2.2. Types of protein analysis

Proteins and peptides can be analyzed by mass spectrometry either in the intact form or as digested protein or peptides. Based on the type of analysis and the form of the proteins being analyzed, the workflow can be categorized as intact/ top-down, middle-up, middle-down, bottom-up.

Top down or intact protein mass spectrometry analysis gives information about the whole protein in its primary confirmation. This approach has the potential to cover the entire protein sequence and fully characterize proteoforms, protein forms resulting from genetic variations and post-translational modifications [94–96].

Bottom-up proteomic analysis involves the introduction of peptides generated by enzymatic cleavage of proteins into the mass spectrometer. The original protein is identified by comparing MS/MS spectra of the peptides generated with the hypothetical peptide MS/MS spectra generated based on the amino acid sequences of proteins in a protein sequence database [96,97].

Middle-down analysis is an emerging approach, which has the potential for successful applications to proteomics. This approach involves the analysis of peptides obtained by proteolysis or chemical degradation of the intact proteins. The size of the analyzed peptides in middle down approach is greater when compared to the peptides in bottom-up approach. This approach results in a relatively lesser number of peptides after proteolytic cleavage in comparison to bottom-up approach leading to a less complicated sample. Longer peptides not only have an advantage of being more unique but also achieve an enhanced sequence coverage of the protein which would allow the detection of more PTMs and proteoforms when compared to the bottom-up approach [96].

Each technique has its own advantages and disadvantages in terms of structural information provided, sequence coverage, sample consumption, and ease of analysis. Often full protein characterizations will be carried out using multiple methods due to their complimentary nature. A brief overview of the different methods is shown in Figure 2.

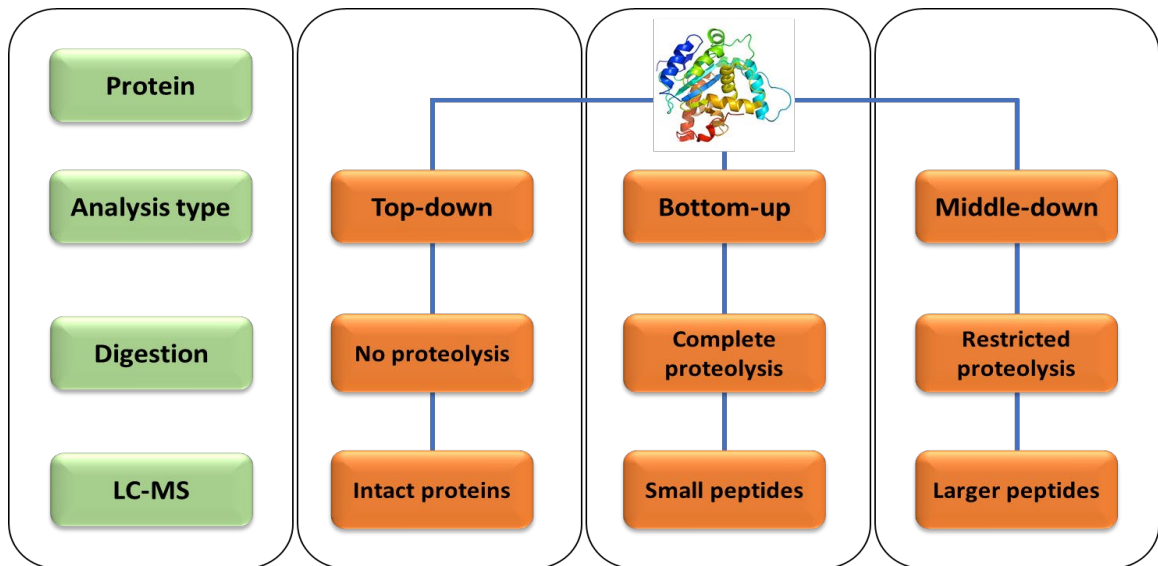


Figure 2: Type of analysis and form of protein analyzed

2.3. Sensitivity considerations for using digesting enzymes

Bottom up proteomics approach (use of surrogate peptide) has become the most used strategy for mass-spectrometry-based protein quantification. The surrogate peptide approach has gained popularity due to the compatibility of the small molecular weight peptides to highly sensitive and specific triple quadrupole mass spectrometers [98,99]

2.4. Types of enzymes used in peptide and protein digestion

Proteolysis is carried out by a group of enzymes called proteases or peptidase, that hydrolyze proteins into constituent peptides. Based on the site of action on the protein, proteases are generally classified as exopeptidases, which target the terminal ends, or as endopeptidases, which target internal peptide bonds. However, proteases are also classified based on their structure and mechanism of action into six major types: aspartic, glutamic, metalloproteases, cysteine, serine, and threonine proteases. A large number of proteases have been identified and reported. The Degradome Database lists 569 human proteases as shown in Table III [100–104].

Table III: Types and number of proteases

S.No.	Type of protease	Number
1	Metalloproteases	194
2	Serine proteases	176
3	Cysteine proteases	150
4	Threonine proteases	28
5	Aspartic proteases	21

Proteases and peptidases have a wide range of industrial, biotechnological and research applications. Applications include: proteolytic digestion of proteins in proteomics studies, peptide synthesis, nucleic acid purification by digesting unwanted proteins, cell culture experiments, exploration of the structure-activity relationships of proteins and peptides and peptide sequencing [105–107].

Enzymatic digestion of the intact proteins is one of the major applications of proteases in proteomics workflow prior to mass spectrometry analysis. Different proteases can be used for the process of digestion based on the requirement of the analysis. A list of few commonly used proteases/peptidases is listed in Table IV [106,108].

Table IV : List of few commonly used proteases along with their cleavage sites

S.No.	Protease/peptidase	Cleavage site
Aspartic		
1	Pepsin	Phe (or Tyr, Leu, Trp)↓Trp (or Phe, Tyr, Leu)
Metalloproteases		
5	Lys N	↓Lys
6	Asp-N	↓Asp
Cysteine		
7	Arg-C	Arg↓
Serine		
9	Trypsin	Arg or Lys↓
10	Chymotrypsin	Trp (or Phe, Leu, Tyr)↓
11	Glu-C	Glu (or Asp)↓
12	Lys-C	Lys↓

The serine protease trypsin is the most widely used enzyme to generate smaller peptides [108,109]. Other proteases such as chymotrypsin, Lys C, Lys N, Asp N, Arg C, and Glu C are also used in addition to trypsin in order to improve the structural identification of proteins [110,111]. The use of proteases/peptidases produces peptides which have a size appropriate for ionization and further detection by mass spectrometry [112].

2.5. Factors affecting the mass spectrometry signal intensity in peptide determination

Sample size and complexity are challenges in mass spectrometry. This can be overcome by careful and target centric sample preparation and increased efficiency of processing. Improving efficiency is important as sample losses during processing can have a huge impact on the sensitivity of the assay. This becomes even more important when processing complex biological matrices due to the extremely low concentrations of analyte.

2.5.1. Instrumentation

Multiple techniques have been developed for the analysis of different kinds of analytes (Table II). The type of instrument to be used for the analysis is decided based on the structure and properties of the analyte. Achievement of lower limits of detection for less abundant intact proteins in a biological sample has been realized from technological advances in mass spectrometer instrumentation. For analysis of intact proteins, a technology such as Fourier Transform Ion Cyclotron Resonance (FT-ICR) provides excellent mass resolution and accuracy, however it lacks the sensitivity required for low level detection of proteins [113]. The advent of orbitrap mass spectrometry improved the ability to detect proteins at low levels [114]. Triple quadrupole (QQQ) mass spectrometers

have a very high sensitivity in the determination of steroids compared to time of flight (TOF) and quadrupole time of flight (QTOF) mass spectrometers [115]. However, QQQ-MS has a lower mass range which is only suitable for low molecular weight proteins and peptide analysis.

2.5.2. Sample preparation

When dealing with protein bioanalysis, sensitivity is one of the major challenges in MS-based assays. All biological matrices have a high abundance of endogenous compounds. These endogenous compounds interfere with the analysis of a protein of interest either by contributing to the background noise or by causing severe ion suppression. This causes a significant reduction in the detection and quantification sensitivity of an assay. An effective sample preparation process that can isolate the protein of interest by reducing the complexity of the sample matrix is thus one of the most important steps in the development of an assay. Many sample preparation techniques have been developed and applied to assay development. One or a combination of different techniques have been applied based on the type of analysis and instruments to be used.

a. Protein precipitation

One of the simplest and widely used sample preparation process is protein precipitation which utilizes water soluble organic solvents such as acetonitrile or methanol to precipitate out large proteins [116,117]. Apart from being simple, this technique has advantages like the ability to remove unwanted proteins from biomatrices prior to LCMS analysis. This process can be used for either extracting organic soluble proteins/peptides [118,119] that are retained in the supernatant or by reconstituting the large proteins which precipitate after addition of an organic phase [119–121].

b. Acidified protein precipitation

This is a modified protein precipitation which is effective to remove high abundant proteins, thereby obtaining a cleaner sample and enhancing the recovery of low abundant proteins [122,123]. Acid-assisted protein precipitation method can efficiently remove albumin which is one of the most abundant proteins, thus making the sample more amenable for analysis of low abundant proteins and peptides [122].

c. Solid-phase extraction (SPE)

This technique has been used more widely in bottom-up proteomics to extract peptides after the digestion step [119,124,125]. Solid-phase extraction is available in multiple formats such as ion-exchange, reverse phase and mixed mode, selected based on the characteristics of the protein/peptide to be extracted. This method has proven effective in removing most large proteins resulting in a relatively cleaner sample to work with. Reversed-phase SPE is used for salt removal; ion-exchange SPE is useful for separation of small proteins and peptides and a mixed mode SPE format has specifically been used in the purification of digested peptides in a matrix [119,125–127].

d. Immunocapture

Sample clean up and extraction of the target peptide from the matrix is one of the major challenges in a sample preparation process. Highly efficient purification and enrichment of the target protein can be achieved using this technique, resulting in an improved detection limit (pg/mL) [128] of the assay [129,130]. Such efficiency makes this the method of choice specially when working with very low abundant proteins and peptides which require a sensitive LCMS assay with low limits of quantification. Stable-isotope standards with capture by anti-peptide antibodies (SISCAPA) technique is one of the

examples of immunocapture that is widely used in bottom-up proteomics to capture a specific surrogate peptide in digested samples [129,130].

e. Selective peptide derivatization

This is a useful technique for qualitative and relative protein quantitative analysis especially when specific immunocapture antibodies are not available for the protein/peptide of interest. Selective surrogate peptides of the protein of interest are derivatized, resulting in a change in the physicochemical properties of the specific target peptides leaving the other peptides in the background underivatized. This change will result in improved separation during extraction and chromatography, and thus enhances sensitivity of LCMS analysis [131].

f. Mobile phase additives

Addition of low percentages (~5%) of dimethyl sulfoxide (DMSO) to mobile phase has been employed for increased electrospray sensitivity. An increase in electrospray efficiency and charge state reduction is due in part to the high proton affinity of DMSO in the gas phase [132–134].

g. Fractionation and separation

A complex biological matrix can be simplified by fractionating the proteins into different groups based on their physical and chemical properties. This technique will reduce the background interference and improve the sensitivity of the assay. A variety of different methods are employed based on the properties of the target analyte that needs to be analyzed. Fractionation of proteins can be designed to separate groups of proteins according to their size, hydrophobicity, charge, isoelectric point, or affinity as shown in Table V [135,136].

Table V : Fractionation methods and dependent physical or chemical property

S.No.	Fractionation method	Physical/ chemical property
1	Ultracentrifugation	Density
2	Size-exclusion chromatography	Stoke's radius
3	Isoelectric focusing	Isoelectric point
4	Hydrophobic interaction chromatography	Hydrophobicity
5	Reversed-phase chromatography	Hydrophobicity
6	Ion-exchange chromatography	Charge
7	Affinity chromatography	Specific biomolecular interaction
8	Gel electrophoresis	Stoke's radius

CHAPTER III

QUANTIFICATION OF DYNORPHINS BY LC-MS: RESULTS AND DISCUSSION

3.1. Analytical background:

Dynorphins are peptides which are present in a very low concentration ranging from 0.16 pg/mL to 23.5 pg/mL in serum [32,33,79]. As these are very potent peptides, the increase in the physiological concentration when stimulated, is relatively low. Immunoassay quantitation is the most utilized technique for determination of dynorphins at physiologic concentrations [34]. Although in the past, LC-MS/MS, MALDI-IMS (imaging mass spectroscopy) and MALDI-TOF methods were developed and afforded the advantage of providing the simultaneous determination of individual dynorphins [83–86], none of these methods were established to quantify the very low physiological concentrations of dynorphins. In this present work, we developed an LC-MS/MS technique using a non-conventional peptidase for the sensitive quantification of dynorphin A, dynorphin B and alpha-neoendorphin.

3.2 Experimental

3.2.1 Chemicals

Dynorphin A (source; Item No. 18169) and dynorphin B (source; Item No. 18178) were from Cayman Chemicals (Ann Arbor, MI, USA), alpha-neoendorphin from NeoScientific (Woburn, MA, USA) and Lys-N endopeptidase from Seikagaku Corporation (Tokyo, Japan). NSA mouse serum from Innovative research, Ammonium bicarbonate (99% analytical grade) was from Sigma-Aldrich (Milwaukee, WI, USA), while dimethyl sulfoxide (DMSO) (HPLC grade) and LCMS grade acetonitrile were from Fisher Scientific (Hampton, NH, USA). Deionized water was from a Nanopore Diamond water purification system from Thermo Scientific (city, state, USA). (missing source of human and mouse serum).

3.2.2 Instrumentation

A Shimadzu Nexera UHPLC system (Columbia, MD, USA) with two LC-30 AD pumps, a Prominence DUG-20A_{3R} degasser, a SIL-30 AC autosampler, a CTO-10AVP column oven and a CBM 20A controller interfaced with an SCIEX 5500 QTRAP mass spectrometer source (Framingham, MA, USA). with an electrospray ionization probe and a syringe pump was used. Instrument operation, acquisition and processing data was performed using SCIEX Analyst software.

3.2.3 Liquid chromatography

A gradient separation technique at room temperature was utilized to separate dynorphin A, dynorphin B and alpha neoendorphin on a Luna Omega Polar C18 100 A LC Column (50 x 1 mm, 1.6 μ m) from Phenomenex (Torrance, CA, USA) with 0.1% formic acid in water as mobile phase A and 0.1% formic acid in acetonitrile as mobile phase B, pumped at a flow rate of 0.20 mL/min. For each analysis, 10 μ L of sample was injected into the system by autosampler set at 10°C. The 17 min gradient run was: 0 % B for 0.5 min, step change to 13.5% B at 0.51 min, holding at 13.5 % B for 8 min, linear gradient to 14% B in 1.5 min, linear gradient to 16% in 2 min, holding 16% B for 3 min and linear gradient to 18% B in 2 min. After the run, the column was washed for 4 min with 80% B and then re-equilibrated with 100% A for 10 min.

3.2.4 Tandem mass spectrometry

A positive electrospray ionization (ESI) mode was used for the mass spectrometric analysis of dynorphin A, dynorphin B and alpha-neoendorphin. A syringe infusion pump at 10 μ L/min of Lys-N-digested peptides (10 pg/ μ L) in 0.1% formic acid and 15% acetonitrile in water was introduced into HPLC effluent of the same composition resulting in a combined flow rate of 0.2 mL/min, in order to optimize mass spectrometer parameters at the HPLC flow rates used. Source parameters for highest signal intensity were as follows: curtain gas 30 psi; ion spray voltage 4500 V; ion spray temperature 400°C; ion source gases (1 and 2) 35 psi; declustering potential 35 V; entrance potential 8 V; collision energy 40 eV and cell exit potential 10 eV.

3.2.5 Preparation of stock and working peptide standards

Stock solution of the three peptides (dynorphin A, dynorphin B and alpha-neoendorphin) were prepared by dissolving the peptide in appropriate volume of 100 % DMSO to obtain concentrations of 1 mg/mL. A volume of 20 uL of the stock solution was aliquoted into 50 vials and stored at -20°C. The working standard solutions of dynorphin A and dynorphin B (1.25, 2.5, 5, 12.5, 25, 250 pg/mL) were prepared from the stock solution by serial dilution with 0.1% formic acid and 2% acetonitrile in water. A stock solution of alpha-neoendorphin was also serially diluted to 50, 75, 100, 125, 250 and 500 pg/mL with 0.1% formic acid and 2% acetonitrile in water. These working standards were then diluted with appropriate volume of pooled mouse serum to prepare the calibrators and quality controls (QCs), as detailed below.

3.2.6 Preparation of serum calibrators and quality control

Calibrators of dynorphin A and dynorphin B (0.125, 0.25, 0.5, 1.25, 2.5, 25 pg/mL) were prepared as described below. A volume of 20 µL each of working standard solution (1.25, 2.5, 5, 12.5, 25, 250 pg/mL) of the peptides was spiked into 180 µL of pooled mouse serum. QCs for dynorphin A (0.375, 12.5 and 20 pg/mL) were prepared by spiking 20 uL of 3.75 pg/mL, 125 pg/mL, and 200 pg/mL standard solution into 180 µL of pooled mouse serum. QCs for dynorphin B were prepared in two batches, first batch of QCs (0.25, 2.5 and 25 pg/mL) were prepared by spiking required concentrations of working standard solution into pooled mouse serum, which was utilized for assessing all validation parameters except matrix effect. The second batch of QCs (0.375, 12.5 and 20 pg/mL) were prepared in six different lots of mouse serum by spiking 20 uL of 3.75 pg/mL, 125 pg/mL,

and 200 pg/mL standard solution into 180 μ L of mouse serum. Calibrators for alpha-neoendorphin (5, 7.5, 10, 12.5, 25, 50 pg/mL) were prepared by spiking 20 μ L each of working standard solution (50, 75, 100, 125, 250 and 500 pg/mL) of the peptides into 180 μ L of pooled mouse serum. QCs for alpha-neoendorphin (10, 25 and 40 pg/mL) were prepared by diluting 20 μ L of 100 pg/mL, 250 pg/mL, and 400 pg/mL standard solution with 180 μ L of pooled mouse serum. Zero calibrator (blank solution) was prepared by spiking 20 μ L of 2% acetonitrile into 180 μ L of pooled mouse serum (n=2). These solutions were further treated as follows to extract the peptides to prepare the final calibrators and QCs. A volume of 900 μ L of 2 % formic acid in ice-cold acetone was added to 40 μ L of spiked mouse serum and shaken at 4°C for 1 h, followed by centrifugation at 17000 g for 15 min at 4°C. The precipitate was separated and 200 μ L of 70% acetonitrile (ACN) containing 12 mM HCl was added to the precipitate and mixed at 4°C for 1 h, then centrifuged at 17000 g for 15 min at 4°C. Low molecular weight proteins and peptides were extracted into the supernatant, which was then transferred into a separate vial. The supernatant was then concentrated using a Centrivap cold trap from Labconco and reconstituted with 40 μ L of 0.1% formic acid and 2% acetonitrile in water.

3.2.7 Digestion of the extracted peptide

A Lys-N endopeptidase stock solution was prepared by dissolving the peptidase in appropriate volume of water to make a 0.1 mg/mL solution. The working solution (500 ng/mL) was prepared by diluting the stock solution with water and stored at -20°C. Digestion buffer (50 mM solution of ammonium bicarbonate and 5 % dimethyl sulfoxide in water) was freshly prepared before every digestion cycle.

Extracted peptide was digested by adding 20 μL of the working Lys-N peptidase solution and 60 μL of digestion buffer to 40 μL of prepared peptide solution (section 3.2.5). This mixture was stirred and incubated at 30⁰C for 12 hours.

3.2.8 Method validation:

The method thus optimized was validated in mouse serum for accuracy, precision, selectivity, lower limit of quantification, matrix effect, recovery and stability to determine its compliance with the limits mentioned in FDA guidelines for bio analytical method validation.

3.2.8.1 Calibration:

The calibration curves were established by plotting the peak area ratios of dynorphin A (y) versus the spiked concentrations (x) of the calibration standards for each of the six calibrators. The slope and correlation coefficient of the calibration curve were calculated linear least squares regression.

3.2.9 Precision, accuracy and absolute extraction recovery:

Intra-assay (within a day) and inter-assay (3 days) precision and accuracy studies were conducted using the three QC standards (n = 3). Accuracy was determined by comparing the concentrations experimentally determined to the concentration of the prepared QCs.

A mean percent recovery was calculated to assess the effect of extraction process on the recovery of the analytes by comparing the experimentally determined peak areas of the peptides post extraction, using pre-extraction spiked QCs standards in serum, with the peak areas of the QC standards spiked into neat solution.

3.2.10 Selectivity, matrix effect and LLOQ:

Six blank serum replicates and six LLOQ serum standards at 0.125 pg/mL were prepared from six different individual lots of mouse serum to evaluate the matrix interference and LLOQ.

A matrix factor was calculated to assess the effect of serum components on dynorphin A, dynorphin B and alpha-neoendorphin. Three QC concentrations were prepared by post extraction addition of the peptides to six individual lots of mouse serum as directed in sections 3.2.5. and 3.2.6. The peak area of the QCs spiked post extraction into serum was compared to the peak area of the QCs in the neat solution.

3.2.11 Stability studies:

Stability studies (n = 3) were done using two different QC concentrations for each of the three dynorphins which were kept at or exposed to the following storage regimens. Dynorphin A: 12 h at room temperature, 6 h and 12 h at autosampler temperature. Dynorphin B: 3 h and 40 h at room temperature, 6 h and 12 h at autosampler temperature and 60-day stability at -20⁰C. Alpha-neoendorphin: 48 h at room temperature and 6 h and 12 h at autosampler temperature. The stability results of these QC standards were compared with theoretical values.

3.3 Results

3.3.1 Results for intact dynorphins

Experiments were done on a-Halo Peptide 2 ES-C18 column (50 x 2.1 mm, 2 μm) (Advanced Material Technology, Chadds Ford, PA, USA), using a mobile phase A of 0.1% formic acid and 10% acetonitrile in water and a mobile phase B of 0.1% formic acid and

90% acetonitrile in a gradient specified below, at a flow rate of 0.40 mL/min. The 15 min gradient run was: 0 % B for 5 min, linear gradient to 90% in 10 min. the column was then washed for 5 min with 90% B. After the run, the column was re-equilibrated with 100% A for 10 min. Source parameters for highest signal intensity were as follows: curtain gas 20 psi; ion spray voltage 5200 V; ion spray temperature 400°C; ion source gases (1 and 2) 35 psi; declustering potential 40 V; entrance potential 5 V; collision energy 60 eV and cell exit potential 15 eV.

Results are given below categorized for each dynorphin.

3.3.1.1 Mass spectrum results for intact dynorphin A

The theoretical mass to charge ratios (m/z) were calculated using the amino acid sequence of dynorphin A and the expected m/z values are shown in Table VI. Three of these ions are seen in the infusion full spectrum mass spectrum given in Figure 3: m/z of 716.8 (+3), 537.8 (+4) and 430.5 (+5).

Table VI : Expected m/z of intact dynorphin A

Possible dynorphin ions from ESI	
Charge state	m/z
+1	2148.5
+2	1074.7
+3	716.8
+4	537.8
+5	430.5

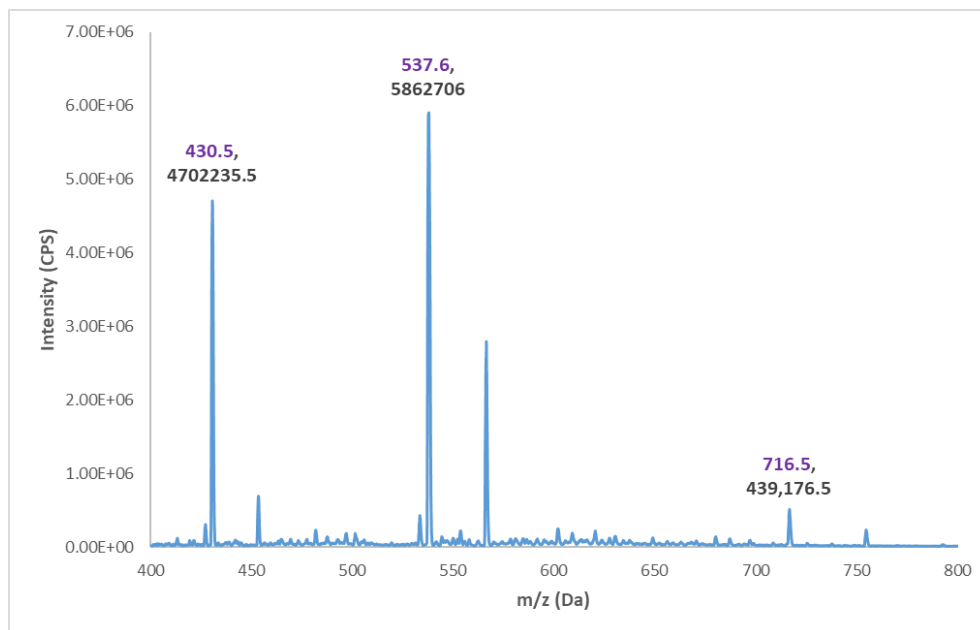


Figure 3 : Full spectrum scan of intact dynorphin A showing the relative intensities of detected m/z at an infusion rate of 10 μ L/minute at 10 pg/ μ L in 15% ACN was infused.

The MS/MS spectra of the parent ions 716.8 (+3), 537.8 (+4) and 430.5 (+5) are shown in Figures 4, 5 and 6 respectively. A syringe infusion pump at 10 μ L/min of intact peptides (10 pg/ μ L) in 0.1% formic acid and 15% acetonitrile in water was introduced, in order to optimize mass spectrometer parameters. Source parameters for highest signal intensity were as follows: curtain gas 30 psi; ion spray voltage 3500 V; ion spray temperature 300°C; ion source gases (1 and 2) 30 psi; declustering potential 35 V; entrance potential 10 V; collision energy 40 eV and cell exit potential 15 eV.

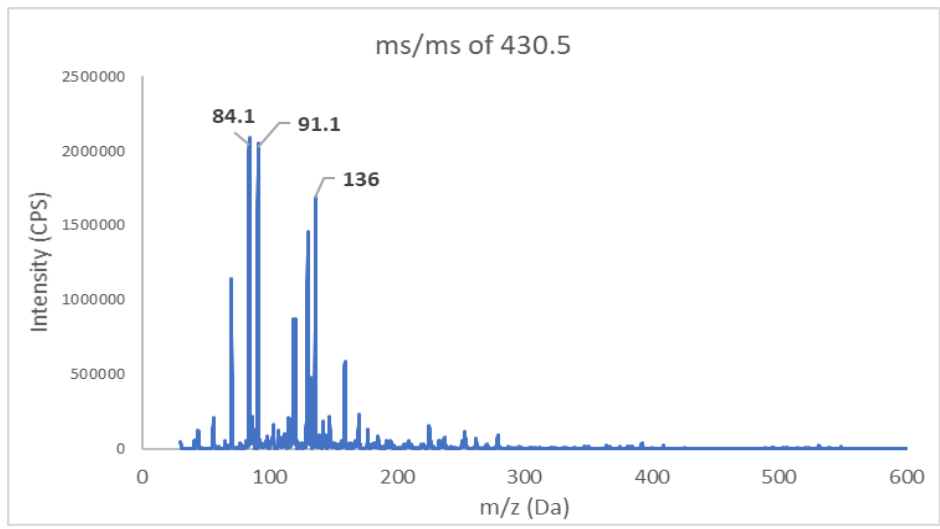


Figure 4 : MS/MS of 430.5 m/z of intact dynorphin A

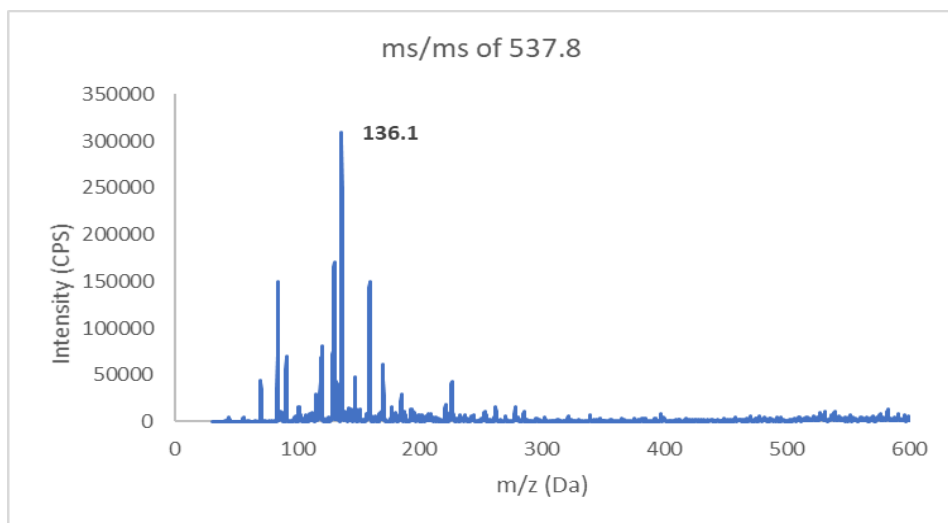


Figure 5 : MS/MS of 537.8 m/z of intact dynorphin A

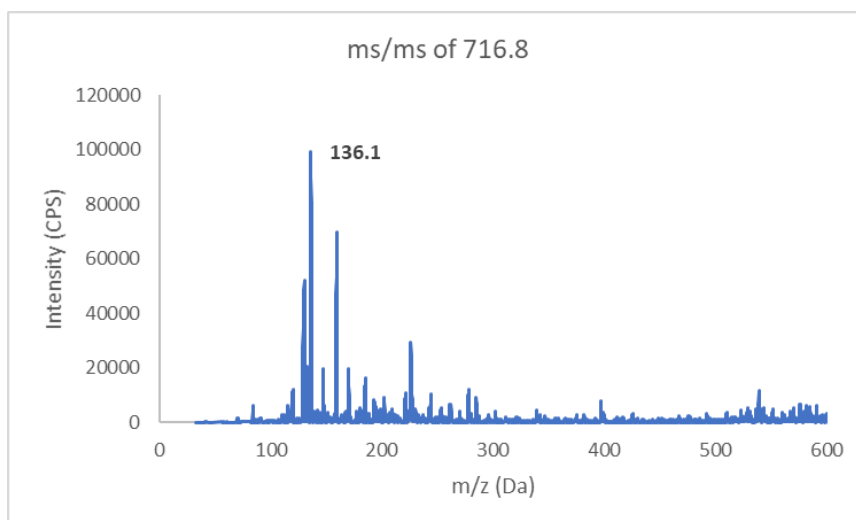


Figure 6 : MS/MS of 716.8 m/z of intact dynorphin A

3.3.1.2 Mass spectrum results for intact alpha-neoendorphin

Preliminary experiments include a full spectrum scan (MS 1 scan) and a MS2 scan for the most intense m/z of the infused intact peptide. The theoretical mass to charge ratios (m/z) were calculated using the amino acid sequence of the peptide and the expected m/z values are shown in Table VII.

The resulting MS/MS spectrum of m/z 410.5 and 615.2 are shown in Figure 7 and Figure 8 respectively. A syringe infusion pump at 10 $\mu\text{L}/\text{min}$ of *intact* peptides (10 $\text{pg}/\mu\text{L}$) in 0.1% formic acid and 15% acetonitrile in water was introduced, in order to optimize mass spectrometer parameters. Source parameters for highest signal intensity were as follows: curtain gas 40 psi; ion spray voltage 5000 V; ion spray temperature 300°C; ion source gases 1 and 2 are 15 and 25 psi respectively; declustering potential 28 V; entrance potential 50 V; collision energy 450 eV and cell exit potential 20 eV.

Table VII : Theoretical m/z values for alpha neoendorphin

Possible alpha neoendorphin ions from ESI	
Charge state	m/z
+1	1229.4
+2	615.2
+3	410.5

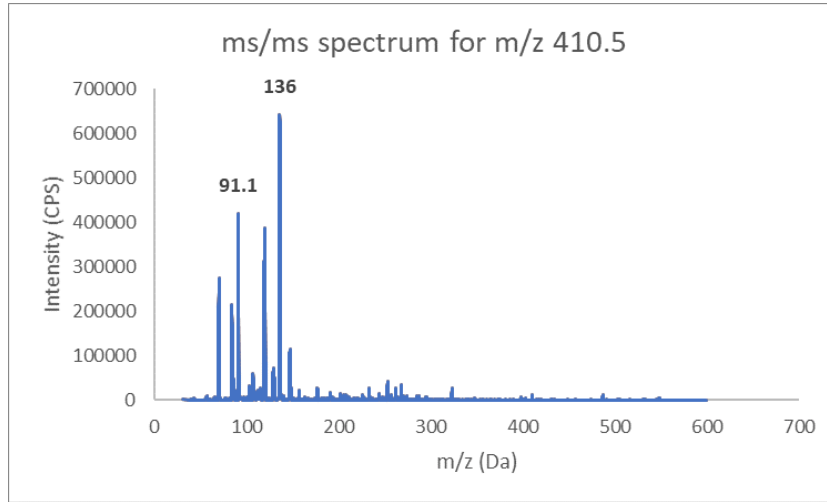


Figure 7 : MS/MS spectrum of 410.5 m/z of intact alpha-neoendorphin

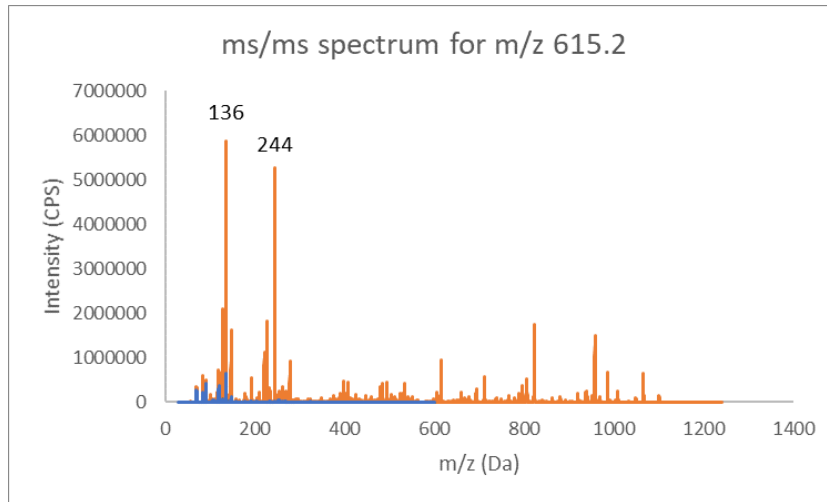


Figure 8 : MS/MS spectrum of 615.2 m/z of intact alpha-neoendorphin

3.3.1.3 LC-MS/MS results of intact dynorphin A and alpha-neoendorphin

Based on the results from the infusion experiments, the combination of the parent and fragment ions (MRM pair) which gave the highest intensity was selected for both dynorphin A and alpha-neoendorphin and are given in Table VIII.

Table VIII : MRM pair for dynorphin A and alpha-neoendorphin

Peptide	Q1 m/z	Q3 m/z
dynorphin A	537.8	136
α-neoendorphin	410	91

LC-MS/MS analysis was performed on a Halo peptide C18 column using the optimized MRM pairs to determine the lower limit of detection (LLOD) and lower limit of quantification (LLOQ) of dynorphin A and alpha-neoendorphin. Chromatograms showing the LLOD of both the peptides is given in Figure 9. The LLOD and LLOQ were found to be 270 pg/mL and 540 pg/mL for dynorphin A and 120 pg/mL and 250 pg/mL for alpha neoendorphin as given in Table IX.

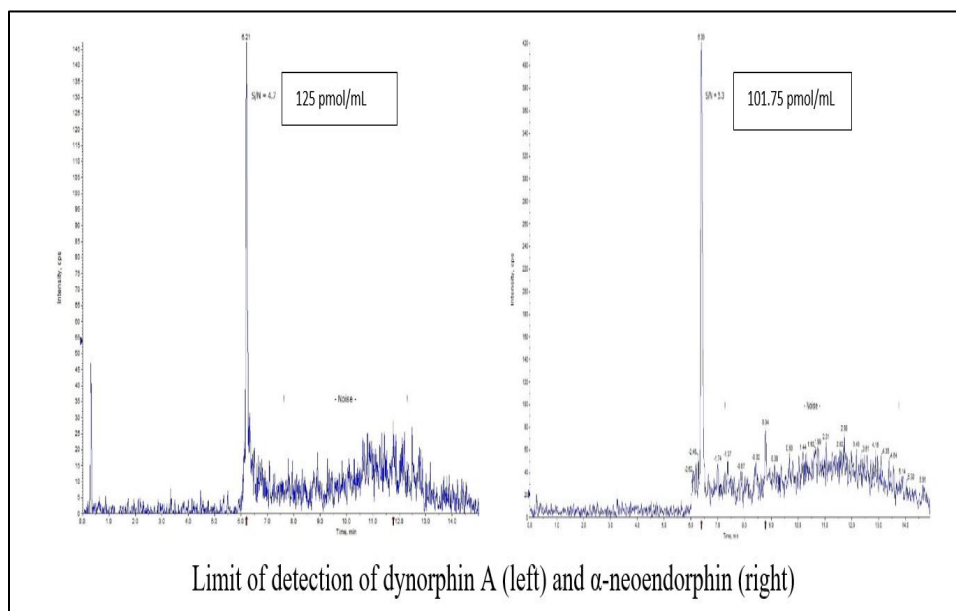


Figure 9 : LLOD of dynorphin A and alpha-neoendorphin

Table IX : LLOD and LLOQ of dynorphin A and alpha neoendorphin

Peptide	LLOD pg/mL	LLOQ pg/mL	Physiologic Conc pg/mL
Dynorphin A	270	540	0.16 to 23.5
α - neoendorphin	120	250	

LLOD: Lower limit of detection

LLOQ: Lower limit of quantification

3.3.1.4 LC-MS/MS conditions:

Concerning the chromatography, extensive studies employing different gradients on two C18 columns were done to optimize the chromatography of dynorphin A and alpha-neoendorphin, however without success in completely resolving the two peptides. Polar end capped C18 columns such as Aquasil C18 (Thermoscientific, Swedesboro, NJ) (50x1 mm, 3 μ m) was one of the column used and the gradient for chromatography started with 0% mobile phase B for the initial 3 minutes, increased to 15.5 % in 0.5 minutes and then to 20 % in 6.5 minutes with a gradient time of 20 minutes in total. A 15-minute wash and equilibration cycle were added after the 20-minute gradient. The overlap of the peptide peaks is shown in Figure 10 for the polar end capped Aquasil C18 column.

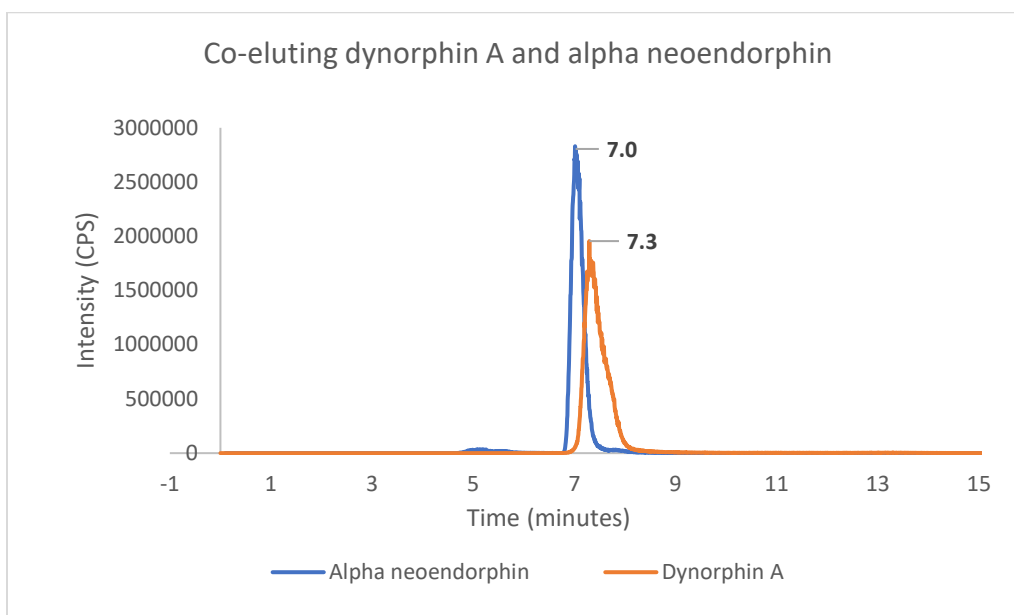


Figure 10 : Co-elution of dynorphin A (mrm pair: 537.8 – 136; 10 pg/ μ L) and alpha-neoendorphin (mrm pair: 410 – 91; 10 g/ μ L) in the LC-MS/MS using an Aquasil C18 column. Injection volume was 20 μ L

3.3.1.5. Discussion of results of intact dynorphins

The results from these experiments gave insight in how the intact peptides respond to mass spectrometry analysis. The following is concluded:

- a. The intact dynorphins were not sensitive to mass spectrometry analysis to determine at physiologic concentrations
- b. Low physiologic concentrations increase the probability of loss of the peptides during the sample preparation process due to nonspecific binding to high abundant proteins in the biological matrix and the walls of the consumables leading to a loss of peptide significantly impacting recovery and reproducibility at such low concentrations.
- c. The peptides, co-eluted and thus optimization of chromatography is needed to not only separate the peptides but also improve sensitivity.

3.3.1.6 Addressing the limitations of intact dynorphin MS analysis

Below is a discussion on what modifications were incorporated in the LC-MS/MS technique to achieve specific and sensitive quantification of dynorphins at physiologic concentrations.

a. Peptide digestion

Digesting a protein/peptide at specific locations of the polypeptide chain based on the proteolytic enzyme specificity. Trypsin is the most used protease in mass spectrometric analysis of peptides and proteins. It cleaves the protein or peptide at the C-terminal side of lysine and arginine amino acid residues. If a proline residue is on the carboxyl side of the cleavage site, the cleavage will not occur. In case of dynorphins, use of trypsin results in

very small peptide fragments which is problematic in MRM techniques in terms of specificity. Fragments that have a longer sequence are more specific for the parent protein/peptide in MRM analysis . Trypsin cleavage sites in dynorphin B are shown in Figure 11.

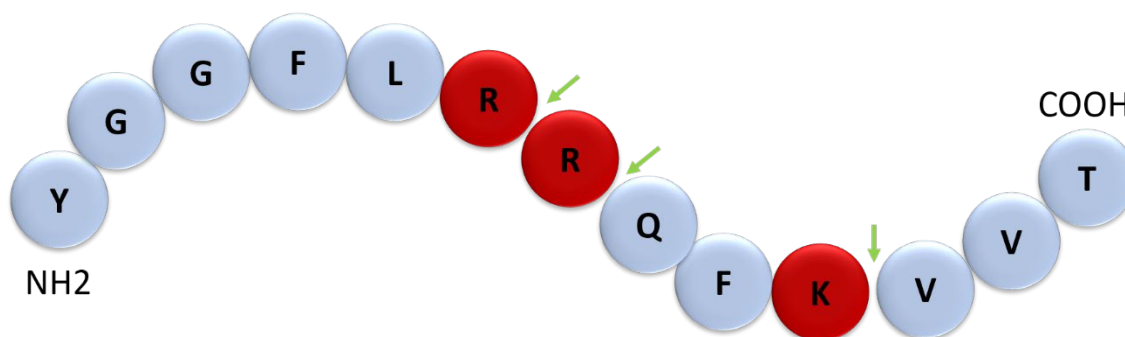


Figure 11 : Trypsin cleavage sites on dynorphin B

To overcome the challenge of generating small nonspecific peptide fragments in trypsin digestion of dynorphins, a novel peptidase called Lys N was used which cleaves the peptides/proteins at the N-terminus of lysine, unless lysine is adjacent to a proline. The expected post digestion peptide fragments of dynorphin A, dynorphin B and alpha-neoendorphin are as shown in Table X. It is noted in Table X that not only are the parent ions different for these three peptides, but also the daughter ions are different, which yields further specificity to the MRM technique. Lys-N cleavage site in dynorphin B is shown in Figure 12, showing the generation of 9 amino acid peptide.

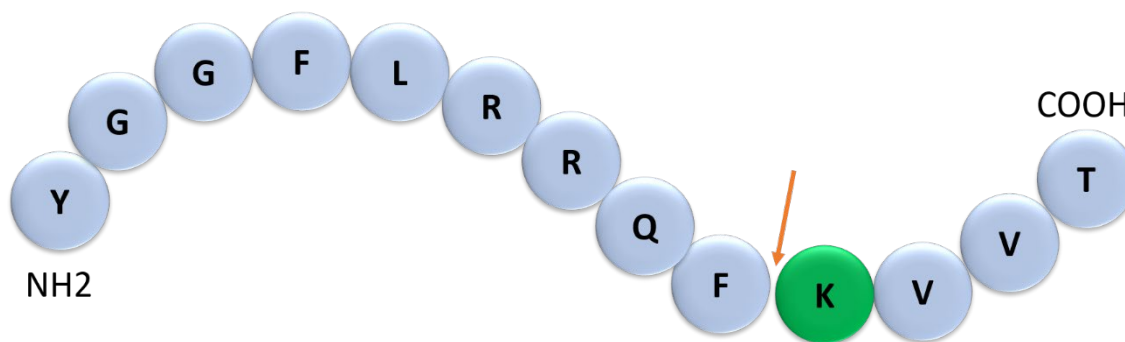


Figure 12 : Lys-N cleavage sites on dynorphin B

Table X : Expected post digestion peptide fragments of dynorphin A, dynorphin B and alpha neoendorphin

Peptide	Sequence and cleavage sites	Generated peptides
Dynorphin A	YGGFLRRIRPKL  KWDNQ	YGGFLRRIRPKL
		KWDNQ
Dynorphin B	YGGFLRRQF  KVVT	YGGFLRRQF
		KVVT
α -neoendorphin	YGGFLR  KYPK	YGGFLR
		KYPK

b. Use of a column with smaller internal diameter

The in-peak concentration of an analyte is dependent on multiple factors such as injection volume, length and internal diameter of the column and retention factor. As shown in the Equation 1, C_{max} increases four-fold when the internal diameter is reduced to half of the original. Based on this, the 2.1 mm internal diameter column used for the initial study was changed to a 1 mm internal diameter column.

$$C_{max} \propto \frac{\sqrt{NV_i}}{Ld_c^2(1+k)} \quad (\text{Equation 1})$$

C_{max} : in-peak concentration

L : length of the column

N : number of plates

d_c : diameterk: retention factor

V_i : injection volume

c. Use of mixed phase column

The reversed phase column that was used for preliminary experiments was replaced with a polar end-capped reversed-phase column [Luna Omega Polar C18 100 A LC column (50 x 1 mm, 1.6 μm)] and a multi-step and extended time gradient was developed in place of a steeper linear gradient which resulted in a baseline of the three dynorphins, as given in the results.

3.3.2 Results for LC-MS/MS of Lys-N digested dynorphins

3.3.2.1 Digestion and chromatographic separation of dynorphins results

Experimental results of digestion performed on the three peptides showed a deviation in the expected cleavage pattern for dynorphin A, as shown in Table XI, with the experimentally determined m/z values given in Table XII.

Table XI : Observed cleavage sites and generated peptides for dynorphin A

Peptide	Sequence and cleavage sites	Generated peptides
Dynorphin A	YGGFLRRIRP  KL  WDNQ	YGGFLRRIRP
		KL
		KWDNQ

Table XII : Amino acid sequence, charge states and molecular weights of the digested peptide fragments
(red highlighted chosen for analysis)

Peptide	Amino acid sequence	Charge state	m/z		
			+3	+2	+1
Dynorphin A	YGGFLRRIRP	+3, +2, +1	412.5	618.2	1234.5
			KL	+1	259.3
	KWDNQ	+1	689.7		
Dynorphin B	YGGFLRRQF	+2, +1	+2	+1	
			572.5	1143.5	
	KVVT	+1	446.5		
Alpha-Neoendorphin	YGGFLR	+1	712.0		
	KYPK	+2, +1	+2	+1	
268.83			535.66		

The separation of peptides dynorphin A, dynorphin B and alpha neendorphin on a Luna Omega Polar C18 100 A LC column is shown in Figure 14.

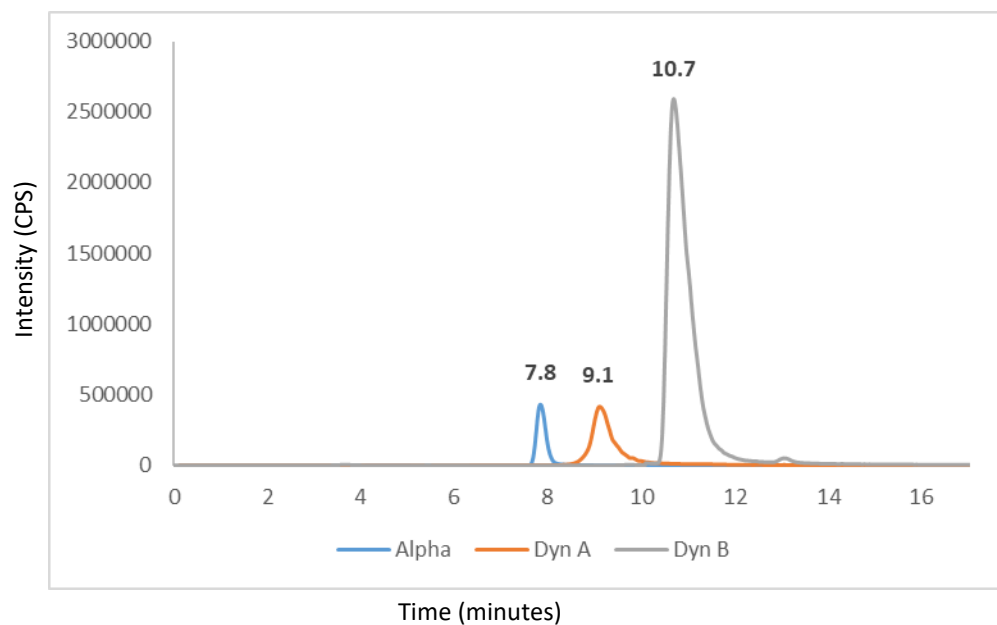


Figure 13 : Separation of the three peptides dynorphin A YGGFLRRIRP fragment (m/z 412 \rightarrow 136), dynorphin B YGGFLRRQF fragment (m/z 572.5 \rightarrow 136.1) and alpha-neoendorphin YGGFLR fragment (m/z 712 \rightarrow 278) on a Luna Omega Polar C18 100 A LC column (25 μ g/mL; Injection volume: 20 μ L)

3.3.2.2 Dynorphin A results

3.3.2.2.1 Liquid chromatogram of dynorphin A

Dynorphin A is a 17 amino acid peptide with five basic amino acids. It forms three fragment peptides after digestion and the retention time of the digested peptide fragment with 10 amino acids (quantifier) is 9.1 minutes (Figure 15).

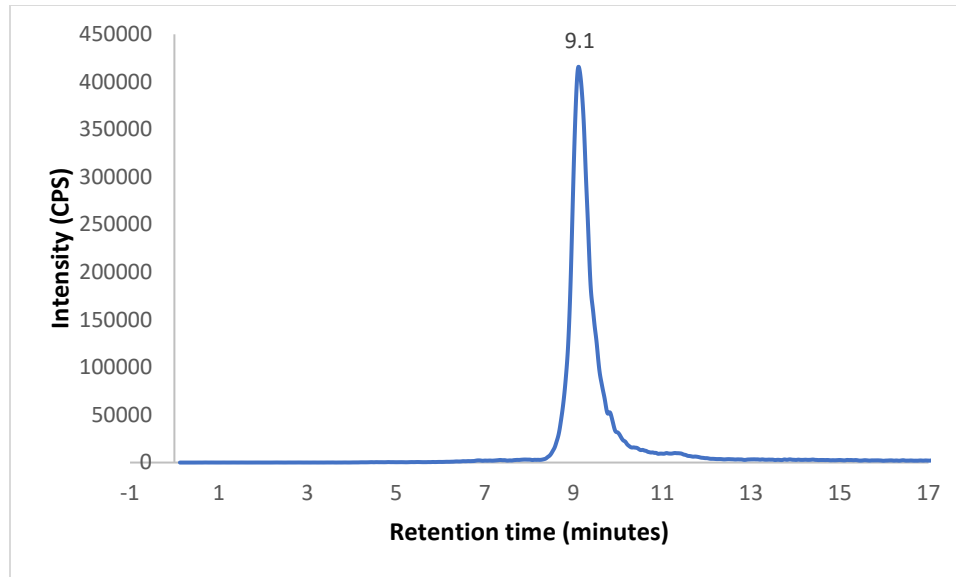


Figure 14 : Chromatogram showing the retention time of dynorphin A YGGFLRRIRP fragment (m/z 412 →136) on a Luna Omega Polar C18 100 A LC column (concentration: 2.5 µg/mL; Injection volume: 20 µL)

3.3.2.2.2 Mass spectrometric detection of dynorphin A

Multiple reaction monitoring (MRM) mode was used for the quantification and specificity of dynorphin A. The selected precursor-product ion pairs for dynorphin A were m/z 412 \rightarrow 136. The mass spectrum of the digested dynorphin A peptide and the ms/ms spectrum of m/z 412 are shown in Figures 16 and 17 respectively.

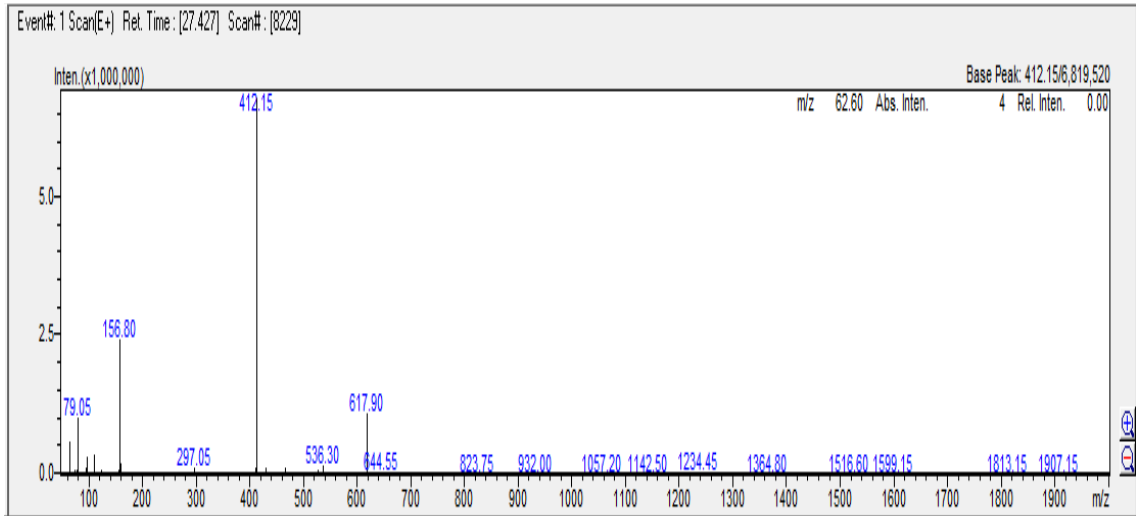


Figure 15 : Infusion mass spectrum of the Lys-N digested fragments of intact dynorphin A

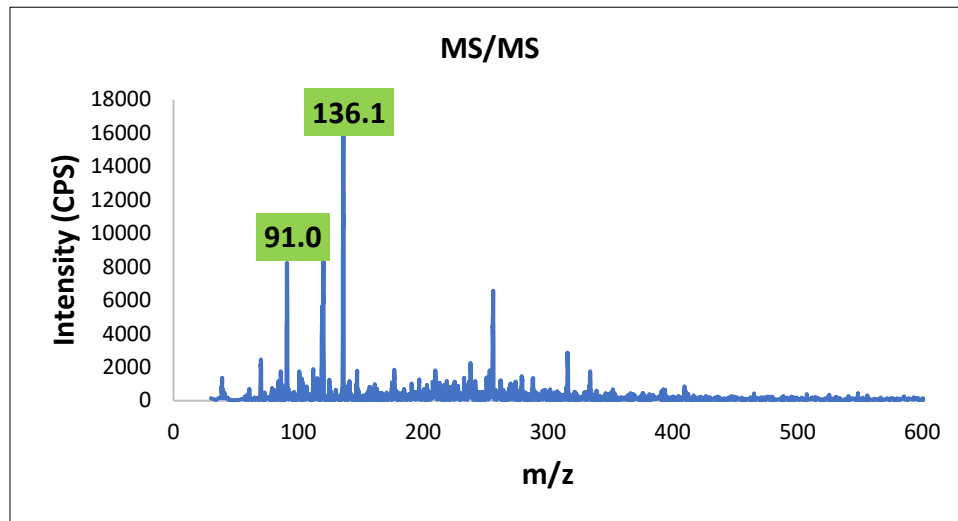


Figure 16 : MS/MS of the daughter ions of digested YGGFLRRIRP fragment of intact dynorphin A

3.3.2.2.3 Method validation of dynorphin A

a. Calibration plot of dynorphin A

Dynorphin A calibration plot of peak areas of the calibrators versus concentration of the intact dynorphin brought through the entire sample preparation steps given in Sections 3.26 and 3.27 using 6 non-zero serum calibrators as shown in Figure 18. The concentrations of the calibrators are 0.125, 0.25, 0.5, 1.25, 12.5 and 25 pg/mL.

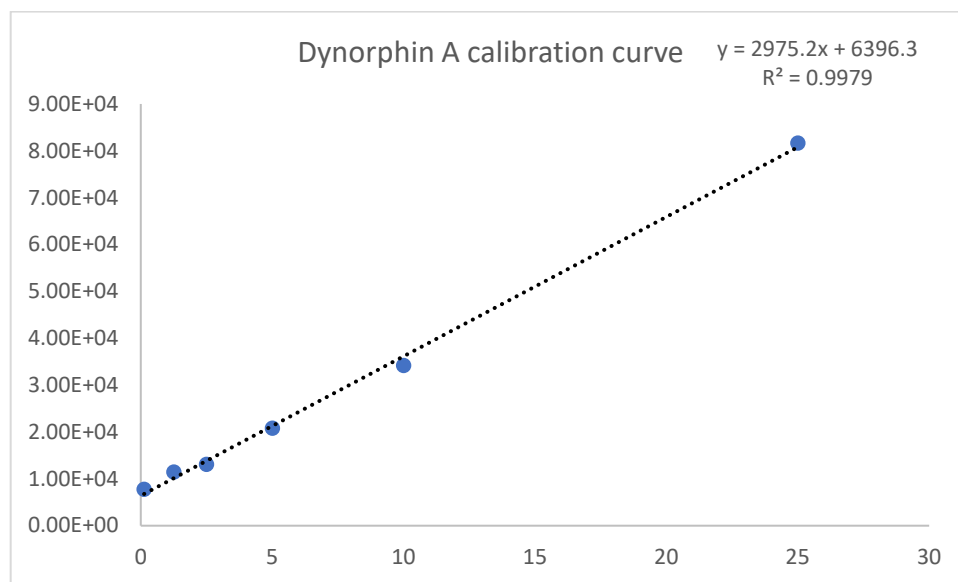


Figure 17 : Calibration plot of intact dynorphin A as measured by the YGGFLRRIRP fragment (m/z 412 →136) in three trials (n=3)

d. Lower limit of quantification of dynorphin A

The lower limit of quantitation (LLOQ) was determined as the concentration of dynorphin A of the lowest calibrator which falls in %CV of 20%. The reproducibility of six replicates in two batches on two separate days of the 0.125 pg/mL calibrator was determined to be a percent coefficient of variance (%CV) of 14% and percent mean relative error was 2% as given in table XIII. The mean peak area of the LLOQ from all the

replicate analysis was $7.44E+03$. The chromatogram for the lowest calibrator concentration is shown in Figure 19.

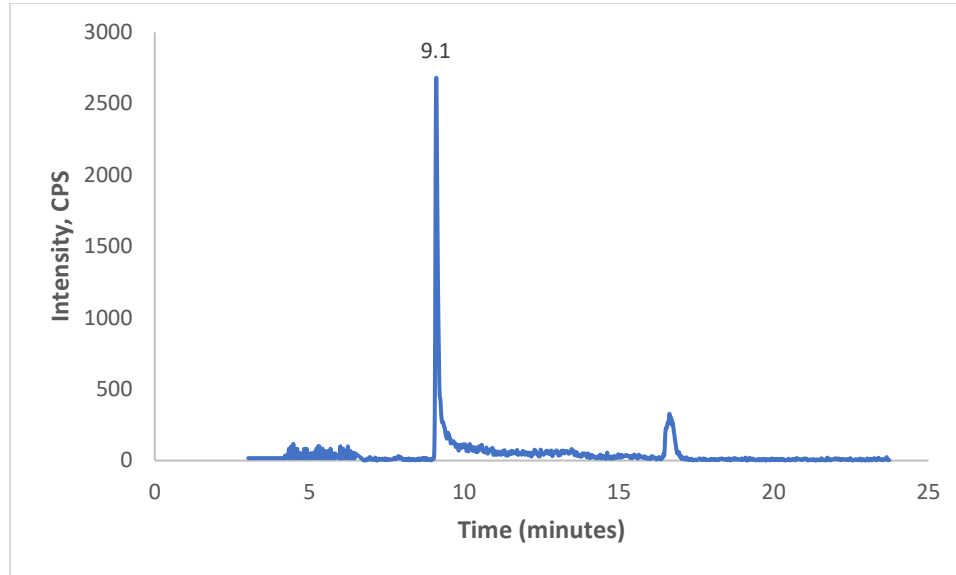


Figure 18 : Chromatogram showing the retention time of dynorphin A YGGFLRRIRP fragment (m/z 412 \rightarrow 136) at the lowest calibrator concentration

Table XIII : Six replicates of 0.125 pg/mL calibrator in 6 lots of mouse serum

	R 1	R 2	R 3	R 4	R 5	R 6	Mean	SD ³	Precision (% CV) ⁴
MC¹ (pg/mL)	0.2	0.1	0.1	0.1	0.1	0.1	0.1	0.0	14
Accuracy (% RE)²	17	3.1	-16	-9.5	9.8	-16	-2.0		

MC¹: Measured concentration

% RE²: Percent relative error

SD³: Standard deviation

% CV⁴: Percent coefficient of variance

R : Replicate

e. Selectivity of dynorphin A

The selectivity of this method was assessed by any interferences observed at the retention times and mass transitions of dynorphin A in six individual blank mouse serum samples. No interferent peak was detected at the same retention time (9.1 minutes) and mass transitions as that of dynorphin A as illustrated by the representative chromatograms of a blank serum in Figure 20.

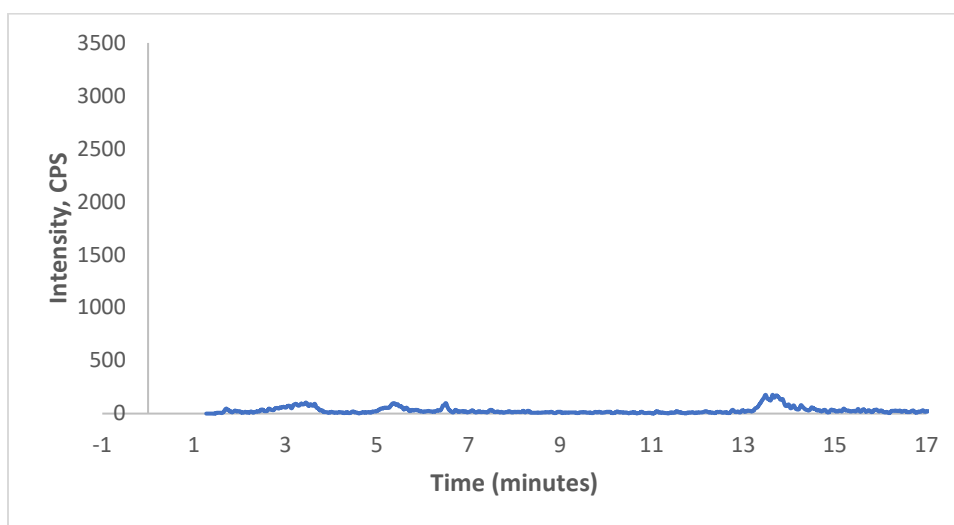


Figure 19 : Chromatogram of the blank serum with MRM set for m/z 412 \rightarrow 136

f. Recovery and matrix effect of dynorphin A

The summarized recovery data of dynorphin A (Table XIV) at three different QC concentrations and LLOQ in pooled mouse serum indicated that the recovery was consistent and within the permissible limits of variability.

Table XIV : Percent recovery and % variance in four concentrations in pooled mouse serum

Prepared Concentration	(MPR \pm SD) ³	%CV ²
0.125	89.4 \pm 0.94	13.8
0.375	89.8 \pm 0.66	11.4
12.5	85.6 \pm 2.63	5.79
25	89.9 \pm 1.79	4.28

CV²: Coefficient of variance (Standard deviation (SD)/Mean calculated concentration)

(MPR \pm SD)³: Mean percent recovery \pm Standard deviation

The mean matrix factor of dynorphin A across all lots and concentrations was 0.87 \pm 0.01. The matrix factor (MF) at three QC concentrations from six different lots of mouse serum is summarized in Table XV.

$$\text{Matrix factor (MF)} = \frac{\text{Peak area post extraction spiked serum samples}}{\text{peak area of the spiked neat solution}} \quad \text{Equation 1}$$

Table XV : Matrix factor (MF) in three concentrations from six different lots of mouse serum

Serum	Nominal Concentration (pg/mL)	MF \pm SD
Lot 1	0.375	0.84 \pm 0.11
	12.50	0.88 \pm 0.05
	20.00	0.89 \pm 0.04
Lot 2	0.375	1.1 \pm 0.11
	12.50	0.87 \pm 0.05
	20.00	0.89 \pm 0.04
Lot 3	0.375	0.85 \pm 0.11
	12.50	0.84 \pm 0.05
	20.00	0.91 \pm 0.04
Lot 4	0.375	0.86 \pm 0.11
	12.50	0.86 \pm 0.05
	20.00	0.92 \pm 0.04
Lot 5	0.375	0.85 \pm 0.11
	12.50	0.91 \pm 0.05
	20.00	0.95 \pm 0.04
Lot 6	0.375	1.1 \pm 0.11
	12.50	0.80 \pm 0.05
	20.00	0.80 \pm 0.04

(ME \pm SD)¹: Matrix Effect \pm Standard deviation

g. Accuracy and precision of dynorphin A

The data for intra-day accuracy and precision were presented in Table XVI and inter-day accuracy and precision are presented in Table XVII. Intra-day accuracy and precision were assessed by three individual replicates of four concentrations on same day while inter-day accuracy and precision were assessed by three replicates of four concentrations on three separate days.

Table XVI : Intra-day accuracy and precision for four concentrations with three replicates on the same day(n=6)

Intra-day accuracy and precision				
Nominal Concentration (pg/ml)	Mean Calculated Concentration (pg/ml)	SD ¹	Precision (% CV) ²	Accuracy (% RE) ³
0.125	0.13	0.02	12.24	-3.14
0.375	0.40	0.02	4.03	-7.98
12.5	11.81	0.52	4.42	5.53
20	20.49	0.48	2.34	-2.44

CV²: Coefficient of variance (Standard deviation (SD)/Mean calculated concentration)

% RE³: Percent relative error

n: calibrators used in calibration plot)

Table XVII : Inter-day accuracy and precision for four concentrations on three different days (n=6)

Inter-day accuracy and precision				
Nominal Concentration (pg/ml)	Mean Calculated Concentration (pg/ml)	SD ¹	Precision (% CV) ²	Accuracy (% RE) ³
0.125	-0.13	0.01	-10.17	6.29
0.375	-0.39	0.02	-4.00	4.60
12.5	-11.64	0.72	-6.19	-6.85
20	-20.10	0.70	-3.48	0.49

CV²: Coefficient of variance (Standard deviation (SD)/Mean calculated concentration)

% RE³: Percent relative error

n: calibrators used in calibration plot)

h. Stability study of dynorphin A

Stability of the QCs of dynorphin A were assessed by analyzing 1 replicate each at two different temperatures (RT: -22°C and 10°C) and the data is summarized in the Table XVIII. Based on the data, dynorphin A is stable for at least 12 hours at benchtop working temperature of -4°C (samples always placed in ice when working on the benchtop), autosampler temperature of 10°C . This data shows that there is a significant loss of the analyte at room temperature, however the loss is not very significant at any of the working temperatures (-4°C - 10°C).

Table XVIII : Stability of dynorphin A at 2 temperatures (-22°C , 10°C)

Stability at room temperature (-22°C)				
	Room temperature		Percent Variance	
Time	PA of the lowest QC	PA of the highest QC	Lowest QC	Highest QC
0 Hours	8.96E+03	7.31E+04		
12 hours	7.72E+03	5.83E+04	-13.88	-20.22
Stability at 10°C				
	Autosampler		Percent Variance	
Time	PA of the lowest QC	PA of the highest QC	Lowest QC	Highest QC
0 Hours	9.09E+03	7.63E+04		
6 hours	9.00E+03	7.60E+04	-0.99	-0.39
12 hours	8.87E+03	7.16E+04	-2.42	-6.16

3.3.2.3 Dynorphin B results

3.3.2.3.1 Liquid chromatogram of dynorphin B

Dynorphin B is a 13 amino acid peptide with 3 basic amino acids. Two peptide fragments are formed after digestion and the retention time of the digested peptide fragment with 9 amino acids (quantifier) is 10.7 minutes (Figure 21).

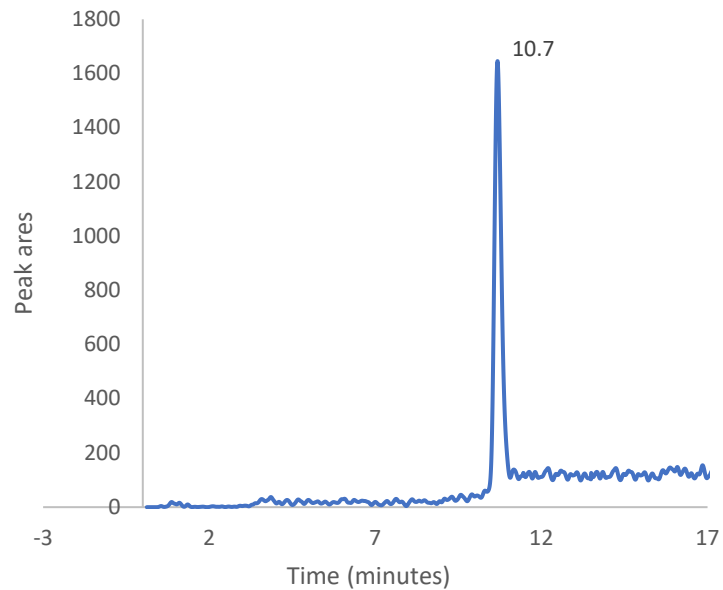


Figure 20 : Chromatogram showing the retention time of dynorphin B YGGFLRRQF fragment (m/z 572.5 \rightarrow 136.1) at the lowest calibrator concentration on a Luna Omega Polar C18 100 A LC column (Injection volume: 20 μ L)

3.3.2.3.2 Mass spectrometric detection of dynorphin B

Multiple reaction monitoring (MRM) mode was used for the quantification and specificity of dynorphin B. The selected precursor-product ion pairs for dynorphin B were m/z 572.5 \rightarrow 136.1. Representative mass spectrum of dynorphin B showing m/z of digested fragment YGGFLRRQF on the top and the ms/ms spectrum of the daughter ion 572.5 on the bottom in Figure 22.

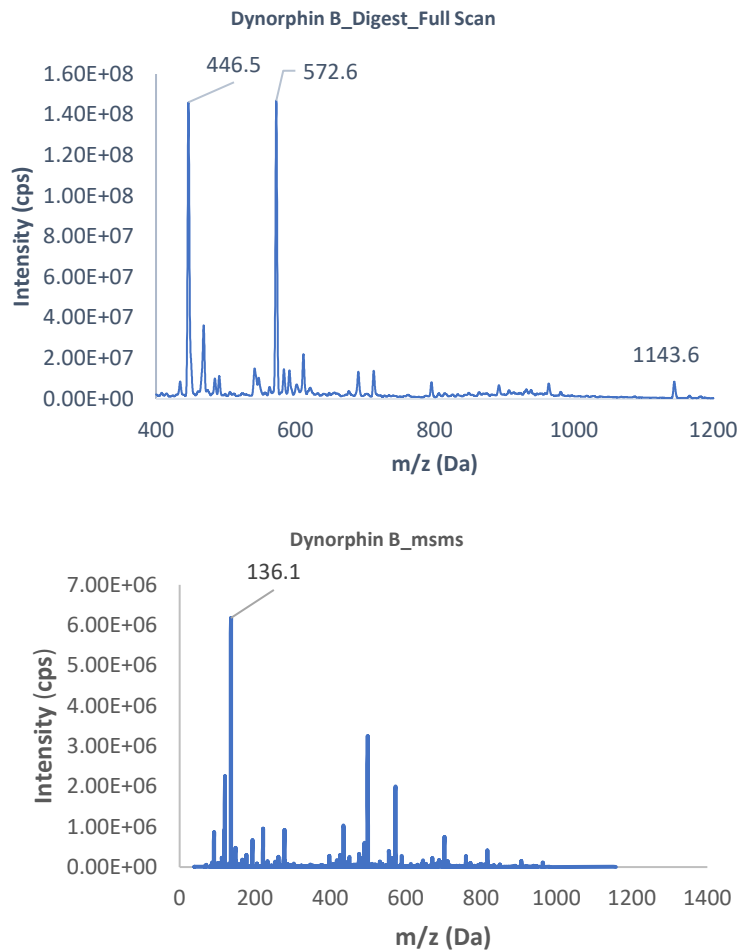


Figure 21 : Infusion mass spectra of dynorphin B showing m/z of Lys-N digested fragment YGGFLRRQF of dynorphin B on the top and the daughter ion of 572.5 on the bottom

3.3.2.3.3 Method validation of dynorphin B

a. Calibration curve of dynorphin B

Dynorphin A calibration plot of peak areas of the calibrators versus concentration of the intact dynorphin brought through the entire sample preparation steps given in Sections 3.26 and 3.27 using 6 non-zero serum calibrators as shown in Figure 23. The concentrations of the calibrators are 0.125, 0.25, 0.5, 1.25, 12.5 and 25 pg/mL

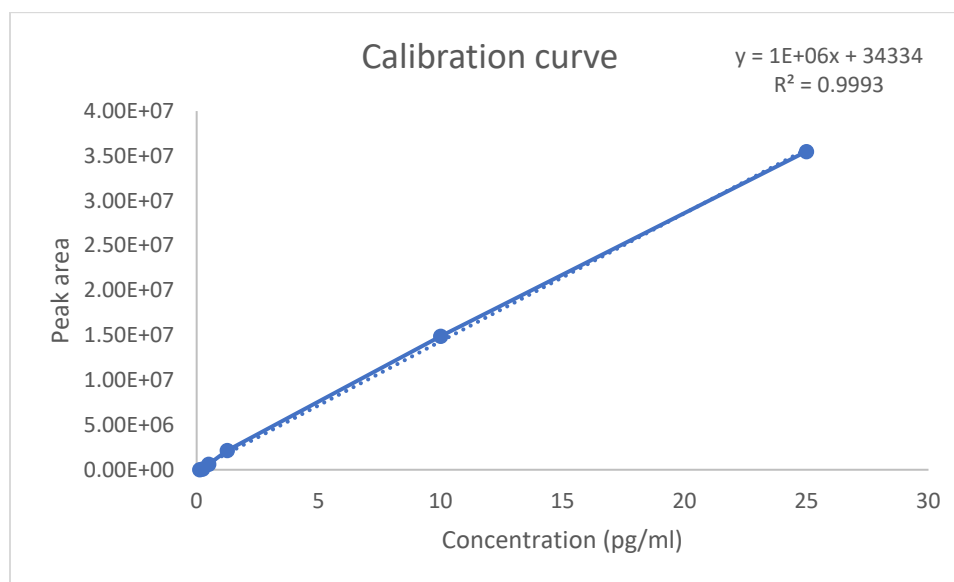


Figure 22 : Calibration plot of intact *dynorphin B* as measured by the YGGFLRRQF fragment (m/z 572.5 \rightarrow 136.1) in three trials ($n=3$)

b. Lower limit of quantification of dynorphin B

The lower limit of quantitation (LLOQ) was determined as the concentration of dynorphin A of the lowest calibrator which falls in %CV of 20%. The reproducibility of six replicates in two batches on two separate days of the 0.125 pg/mL calibrator was determined to be a percent coefficient of variance (%CV) of 9.2 % and percent mean relative error was 1.7 % as given in table XIX. The mean peak area of the LLOQ from all

the replicate analysis was 3.26E+04. The chromatogram for the lowest calibrator concentration is shown in Figure 24.

Table XIX : Six replicates of 0.125 pg/mL calibrator in 6 lots of mouse serum

	R 1	R 2	R 3	R 4	R 5	R 6	Mean	SD³	Precision (% CV)⁴
MC¹ (pg/mL)	0.14	0.12	0.14	0.12	0.12	0.12	0.13	0.012	9.2
Accuracy (% RE)²	-12	6.8	-12	0.81	5.9	4.2	-1.7		

MC¹: Measured concentration

% RE²: Percent relative error

SD³: Standard deviation

% CV⁴: Percent coefficient of variance

R : Replicate

c. Selectivity of dynorphin B

The selectivity of this method was assessed by any interferences observed at the retention times and mass transitions of dynorphin B in five individual blank mouse serum matrices. A tiny endogenous interferent peak was detected at the same retention time (10.7 minutes) and mass transitions as that of dynorphin B as illustrated by the representative chromatograms of the blank serum (Figure 25). The mean peak area of the endogenous interferent from five different individual blank serum injections was found to be 7.3 % of the mean peak area of dynorphin B at the LLOQ (table XX), which was lower than the 20% limit set by US Food and Drug Administration. The chromatogram representing the LLOQ is shown in Figure 24.

Table XX : Selectivity and Lower limit of quantification

Sample Name	Mean Peak Area (counts)	Ratio	Percent
LLOQ ¹ _1	3.26E+04	14	
Blank	2.36E+03		7.3

LLOQ¹: Lower limit of quantification

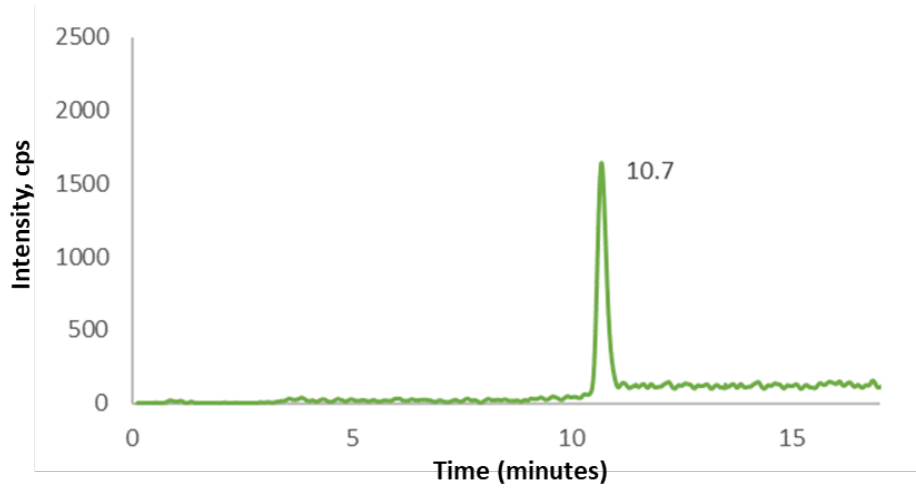


Figure 23 : Chromatogram showing the retention time of Lys-N digested fragment dynorphin B YGGFLRRQF fragment (m/z 572.5 \rightarrow 136.1) at the lower limit of quantification

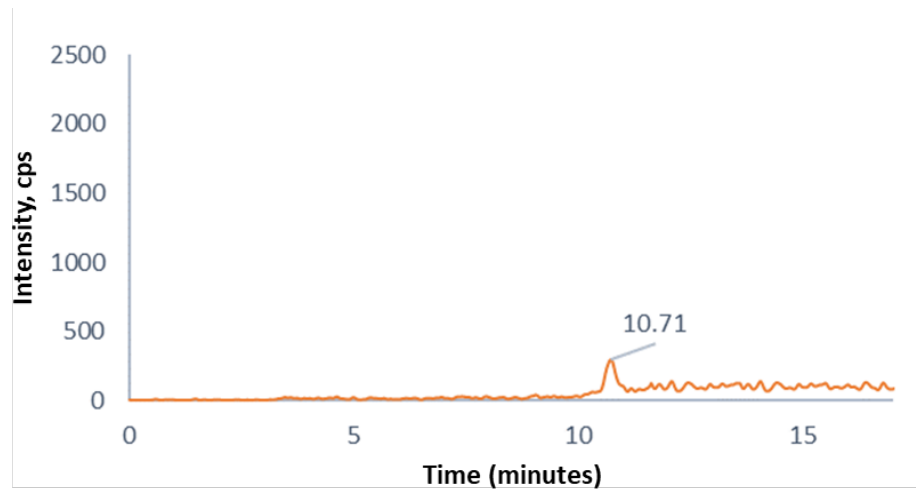


Figure 24 : Chromatogram showing the small interferant peak retention time of Lys-N digested fragment dynorphin B YGGFLRRQF fragment (m/z 572.5 \rightarrow 136.1)

d. Recovery and matrix effect of dynorphin B

The summarized recovery data of dynorphin B as shown in Table XXI at three different QC concentrations and LLOQ in pooled mouse serum indicated that the recovery was consistent and within the permissible limits of variability.

Table XXI : Percent recovery and % variance in four concentrations from six different replicates of pooled mouse serum

Nominal Concentration	(MPR ± SD) ³	%CV ²
0.125	91 ± 2.7	2.7
0.5	93 ± 0	0
1.25	101 ± 3.5	3.5
25	85 ± 6.2	6.2

CV²: Coefficient of variance (Standard deviation (SD)/Mean calculated concentration)
(MPR ± SD)³: Mean percent recovery ± Standard deviation

The mean matrix factor of dynorphin B across all lots and concentrations was 1.01±0.11. It can thus be inferred from the data that there was a signal enhancement effect which may be due the presence of an interferant peak at the retention time (10.7 minutes) of dynorphin B. The matrix factor (MF) at three QC concentrations from six different lots of mouse serum is summarized in Table XXII.

$$\text{Matrix factor (MF)} = \frac{\text{Peak area post extraction spiked serum samples}}{\text{peak area of the spiked neat solution}}$$

Table XXII : Matrix factor (MF) in three concentrations from six different lots of mouse serum

Serum	Nominal Concentration	MF \pm SD
Lot 1	0.125	1.07 \pm 0.13
	2.5	1.05 \pm 0.13
	25	1.01 \pm 0.01
Lot 2	0.125	1.01 \pm 0.13
	2.5	1.12 \pm 0.13
	25	1.01 \pm 0.01
Lot 3	0.125	1.18 \pm 0.13
	2.5	1.04 \pm 0.13
	25	1.01 \pm 0.01
Lot 4	0.125	0.97 \pm 0.13
	2.5	0.88 \pm 0.13
	25	1.0 \pm 0.01
Lot 5	0.125	0.89 \pm 0.13
	2.5	0.83 \pm 0.13
	25	0.99 \pm 0.01
Lot 6	0.125	0.87 \pm 0.13
	2.5	0.83 \pm 0.13
	25	0.98 \pm 0.01

(ME \pm SD)¹: Matrix Effect \pm Standard deviation

e. Accuracy and precision of dynorphin B

Intraday accuracy and precision were assessed by three replicates of four concentrations on same day as summarized in table XXIII while inter-day accuracy and precision were assessed by three replicates of four concentrations on three separate days as summarized in table XXIV.

Table XXIII : Intra-day accuracy and precision for four concentrations with three replicates on the same day(n=6)

Intraday accuracy and precision				
Nominal Concentration (pg/ml)	Mean Calculated Concentration (pg/ml)	SD ¹	Precision (% CV) ²	Accuracy (% RE) ³
0.125	0.13	0.01	10.8	-6.93
0.5	0.57	0.01	1.52	-14.0
2.5	2.52	0.07	2.65	-0.67
25	24.6	0.69	2.82	1.60

CV²: Coefficient of variance (Standard deviation (SD)/Mean calculated concentration)

% RE³: Percent relative error

n: calibrators used in calibration plot)

Table XXIV : Inter-day accuracy and precision for four concentrations with three replicates on three different days (n=6)

Inter-day accuracy and precision				
Nominal Concentration (pg/ml)	Mean Calculated Concentration (pg/ml)	SD ¹	Precision (% CV) ²	Accuracy (% RE) ³
0.125	0.13	0.00	2.40	-1.73
0.5	0.53	0.02	3.15	-6.63
2.5	2.49	0.01	0.23	0.33
25	24.4	0.85	3.49	2.47

CV²: Coefficient of variance (Standard deviation (SD)/Mean calculated concentration)

% RE³: Percent relative error

n: calibrators used in calibration plot)

f. Stability study of dynorphin B

Stability of the QCs of dynorphin B were assessed by analyzing 1 replicate each at three different temperatures (22⁰C, 10⁰C, -20⁰C) and the data is summarized in the Table XXV. Based on the data, dynorphin B is stable for at least 12 hours at benchtop working temperature of -4⁰C (samples always placed in ice when working on the benchtop), autosampler temperature of 10⁰C and for 60 days at the storage temperature of -20⁰C.

This data shows that there is a significant loss of the analyte at room temperature, however the loss is not very significant at any of the working temperatures (-4°C - 10 °C). The data for the stability of dynorphin B is summarized in table XXV.

Table XXV : Stability of dynorphin B at three temperatures (-22 °C, 10°C, -20°C)

Stability at room temperature (-22 °C)				
	Room temperature		Percent Recovery (loss of analyte)	
Time	PA of the lowest QC	PA of the highest QC	Lowest QC	Highest QC
0 hours	7.09E+03	1.61E+05		
3 hours	4.29E+03	1.36E+05	39.49	15.53
40 hours	2.09E+03	6.67E+03	70.52	95.86
Stability at 10 °C				
	Autosampler		Percent Variability (loss of analyte)	
Time	PA of the lowest QC	PA of the highest QC	Lowest QC	Highest QC
0 hours	1.53E+03	1.19E+04		
6 hours	1.41E+03	1.13E+04	7.84	5.04
12 hours	1.35E+03	1.14E+04	4.26	0.88
Long term stability (-20 °C)				
	Calculated Concentrations		Percent Variability (loss of analyte)	
Time	Lowest QC	Highest QC	Lowest QC	Highest QC
0 hours	0.129	23.2	10.08	7.33
60 days	0.142	21.5		

PA: Peak area

3.3.2.4 Alpha-neoendorphin results

3.3.2.4.1 Liquid chromatogram of alpha-neoendorphin

Alpha neoendorphin is a ten amino acid peptide with three basic amino acids. Two peptide fragments are formed after digestion and the retention time of the digested peptide fragment with six amino acids (quantifier) is 7.8 minutes as shown in Figure 26.

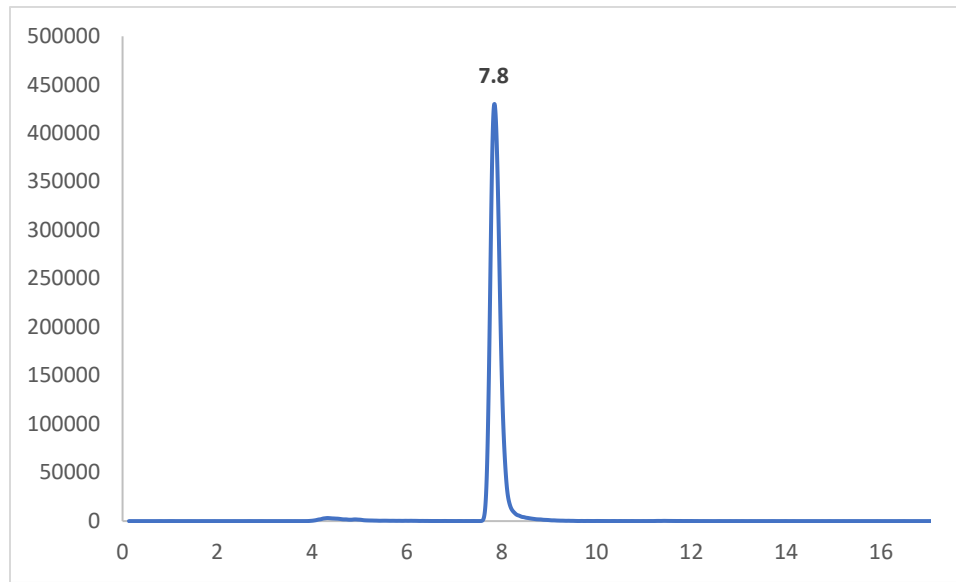


Figure 25 : Chromatogram showing the retention time of Lys-N digested alpha-neoendorphin fragment YGGFLR (m/z 712 →278) at the highest calibrator concentration on a Luna Omega Polar C18 100 A LC column, Injection volume: 20 µL

3.3.2.4.2 Mass spectrometric detection alpha-neoendorphin

Multiple reaction monitoring (MRM) mode was used for the quantification and specificity of alpha neoendorphin. The selected precursor-product ion pairs for alpha neoendorphin were m/z 712 \rightarrow 278. The infusion mass spectrum of the Lys-N digested alpha-neoendorphin peptide (YGGFLR) and the ms/ms spectrum of m/z 712 are shown in Figure 27 and figure 28 respectively.

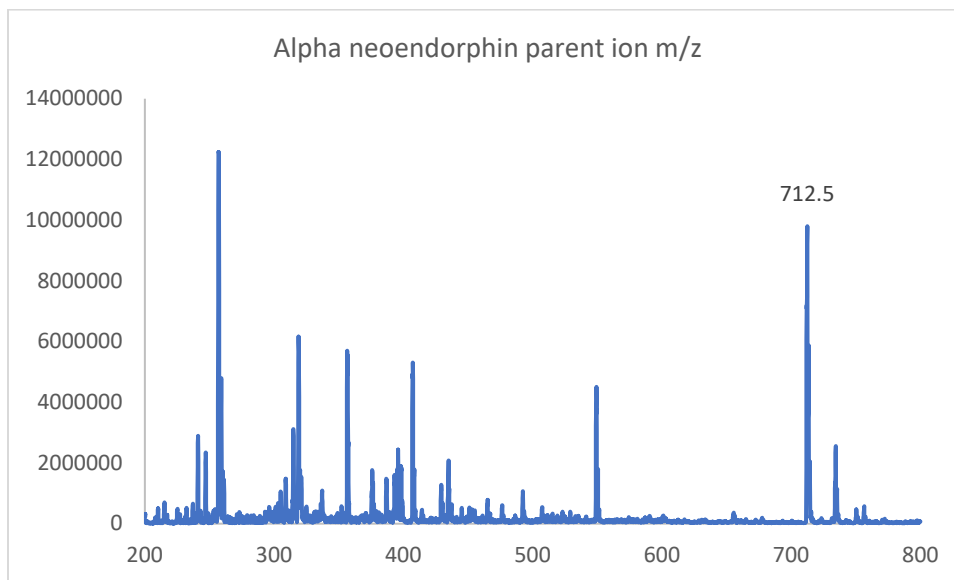


Figure 26 : Infusion mass spectra of the Lys-N digested fragments of intact alpha-neoendorphin (YGGFLR: m/z 712)

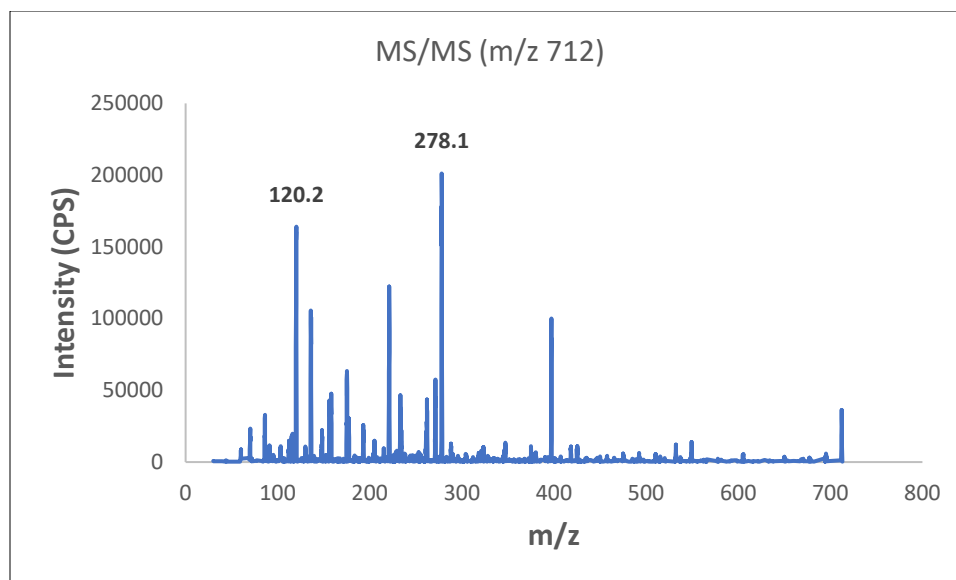


Figure 27 : *MS/MS spectrum of the daughter ions of digested YGGFLR (m/z 712) fragment of intact alpha-neoendorphin*

3.3.2.4.3 Method validation of alpha-neoendorphin

a. Calibration plot of alpha-neoendorphin

Alpha-neoendorphin calibration plot of peak areas of the calibrators versus concentration of the intact alpha-neoendorphin brought through the entire sample preparation steps given in Sections 3.26 and 3.27 using 6 non-zero serum calibrators as shown in Figure 29. The concentrations of the calibrators are 5, 7.5, 10, 12, 25 and 50 pg/mL.

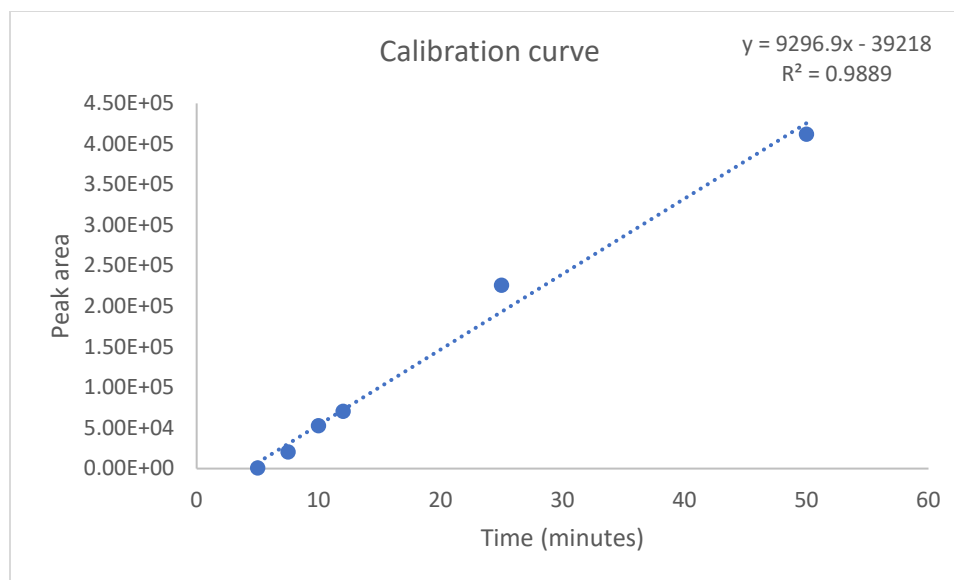


Figure 28 : Calibration plot of intact alpha-neoendorphin as measured by the YGGFLR (m/z 712 →278) in three trials (n=3)

b. Lower limit of quantification of alpha-neoendorphin of alpha-neoendorphin

The lower limit of quantitation (LLOQ) was determined as the concentration of alpha-neoendorphin at the lowest calibrator (5 pg/mL) which falls in %CV of 20%. The reproducibility of six replicates in two batches on two separate days of the 5 pg/mL calibrator was determined to be a percent coefficient of variance (%CV) and percent mean relative error was 13% as given in table XXVI. The chromatogram for the lowest calibrator concentration is shown in Figure 30.

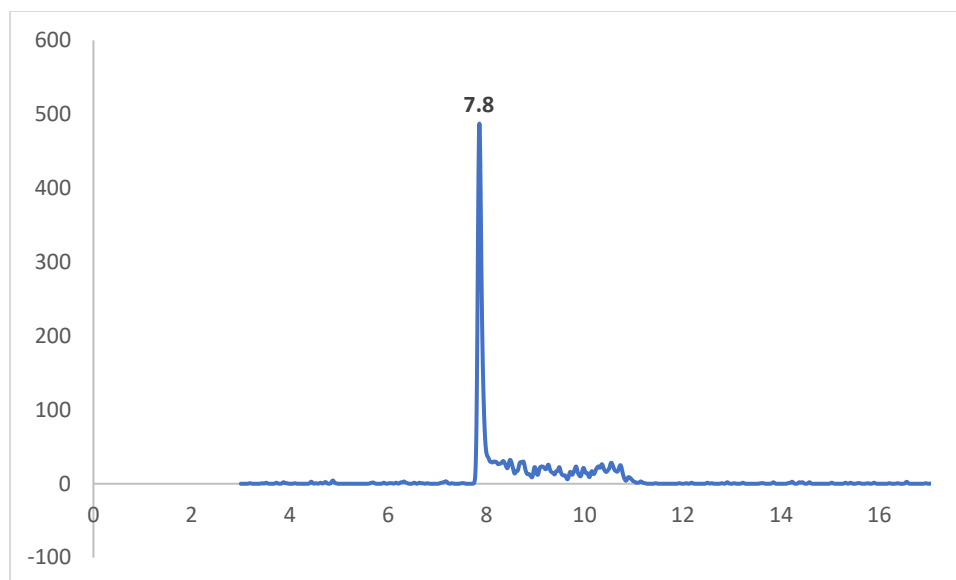


Figure 29 : Chromatogram showing the retention time of alpha neendorphin digested fragment YGGFLR (m/z 712 →278) at the lower limit of quantification

Table XXVI: Six replicates of 0.125 pg/mL calibrator in 6 lots of mouse serum

	R 1	R 2	R 3	R 4	R 5	R 6	Mean	SD ³	Precision (% CV) ⁴
MC¹ (pg/mL)	5.7	5.7	4.4	4.5	5.8	5.9	-5.3	0.69	-13
Accuracy (% RE)²	13	14	-11	-10	18	18	13		

MC¹: Measured concentration
 % RE²: Percent relative error
 SD³: Standard deviation
 % CV⁴: Percent coefficient of variance
 R : Replicate

c. Selectivity of alpha-neoendorphin of alpha-neoendorphin

The selectivity of this method was assessed by any interferences observed at the retention times (7.8 minutes) and mass transitions of alpha-neoendorphin in six individual blank mouse serum samples. No interfering peak was detected at the same retention time (7.8 minutes) and mass transitions as that of alpha-neoendorphin A as illustrated by the representative chromatograms of a blank serum in Figure 31.

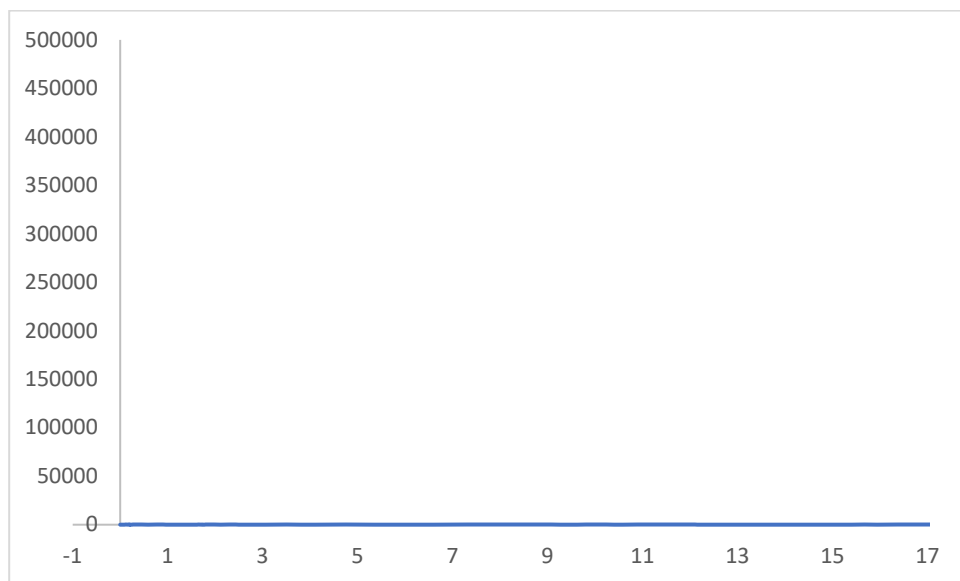


Figure 30 : Chromatogram of the blank serum showing no interfering peak when analyzed for Lys-N digested fragment YGGFLR of intact alpha-neoendorphin analyzed for mrm of 712 →278

i. Recovery and matrix effect of alpha-neoendorphin

The summarized recovery data of alpha-neoendorphin (Table XXVII) at three different QC concentrations and LLOQ in pooled mouse serum indicated that the recovery was consistent and within the permissible limits of variability.

Table XXVII : Percent recovery and % variance in four concentrations in pooled mouse serum

Nominal Concentration (pg/mL)	(MPR ± SD) ³	%CV ²
40	86.9 ± 0.62	0.01
10	86.7 ± 0.80	0.01
5	82.5 ± 2.62	0.03

CV²: Coefficient of variance (Standard deviation (SD)/Mean calculated concentration)

(MPR ± SD)³: Mean percent recovery ± Standard deviation

The mean matrix factor of dynorphin A across all lots and concentrations was 0.84 ± 0.41. The matrix factor (MF) at three QC concentrations from six different lots of mouse serum is summarized in Table XXVIII.

$$\text{Matrix factor (MF)} = \frac{\text{Peak area post extraction spiked serum samples}}{\text{peak area of the spiked neat solution}}$$

Table XXVIII : Matrix factor (MF) in three concentrations from six different lots of mouse serum

Serum	Nominal Concentration (pg/mL)	MF \pm SD
Lot 1	40	0.87 \pm 0.15
	25	0.88 \pm 0.08
	10	0.87 \pm 0.29
Lot 2	40	0.88 \pm 0.15
	25	0.97 \pm 0.08
	10	0.87 \pm 0.29
Lot 3	40	0.99 \pm 0.15
	25	0.89 \pm 0.08
	10	1.35 \pm 0.29
Lot 4	40	0.92 \pm 0.15
	25	0.99 \pm 0.08
	10	1.11 \pm 0.29
Lot 5	40	1.19 \pm 0.15
	25	0.81 \pm 0.08
	10	1.55 \pm 0.29
Lot 6	40	1.20 \pm 0.15
	25	0.81 \pm 0.08
	10	1.42 \pm 0.29

(ME \pm SD)¹: Matrix Effect \pm Standard deviation

j. Accuracy and precision of alpha-neoendorphin

The accuracy and precision of the method was evaluated by analyzing replicates of QCs in pooled mouse serum at 5, 10, 25 and 40 pg/mL on the same day (intra-assay) and 3 separate days (inter-assay). The data for intraday-assay accuracy and precision were presented in Table XXIX and interday-assay accuracy and precision were presented in Table XXX. Intraday accuracy and precision were assessed by 3 replicates of 4 concentrations on same day while inter-day accuracy and precision were assessed by 3 replicates of 4 concentrations on 3 separate days.

Table XXIX : Intra-day accuracy and precision for four concentrations with three replicates on the same day(n=6)

Intraday accuracy and precision				
Prepared Concentration (pg/ml)	Mean Calculated Concentration (pg/ml)	SD ¹	Precision (% CV) ²	Accuracy (% RE) ³
40	0.13	0.01	0.20	-14.65
25	0.26	0.02	1.64	-8.30
10	0.57	0.01	0.03	-14.82
5	1.18	0.13	0.00	13.45

Table XXX : Inter-day accuracy and precision for four concentrations on three different days (n=6)

Inter-day accuracy and precision				
Prepared Concentration (pg/ml)	Mean Calculated Concentration (pg/ml)	SD ¹	Precision (% CV) ²	Accuracy (% RE) ³
40	39.56	5.04	12.73	-1.11
25	23.20	1.47	6.33	-7.19
10	9.59	0.99	10.31	-4.13
5	5.33	0.78	14.57	6.62

CV²: Coefficient of variance (Standard deviation (SD)/Mean calculated concentration)

% RE³: Percent relative error

k. Stability study of alpha-neoendorphin

Stability of the QCs of alpha-neoendorphin were assessed by analyzing 1 replicate each at two different temperatures (RT: -22°C and 10°C) and the data is summarized in the Table XXXI. Based on the data, dynorphin A is stable for at least 12 hours at benchtop working temperature of -4°C (samples always placed in ice when working on the benchtop), autosampler temperature of 10 °C. This data shows that there is a significant loss of the analyte at room temperature, however the loss is not very significant at any of the working temperatures (-4°C - 10 °C).

Table XXXI : Stability of alpha neoendorphin at 2 temperatures (-22 °C, 10°C)

Stability at room temperature (-25 °Cs)				
	Room temperature		Percent Variability	
Time	PA of the lowest QC	PA of the highest QC	Lowest QC	Highest QC
0 Hours	3.36E+03	4.99E+05		
48 hours	1.39E+03	4.27E+05	-58.63	-14.43
Stability at 10 °C				
	Autosampler		Percent Variability	
Time	PA of the lowest QC	PA of the highest QC	Lowest QC	Highest QC
0 Hours	1.74E+03	4.50E+05		
6 hours	1.73E+03	4.41E+05	-0.58	-2.04
12 hours	1.65E+03	4.46E+05	-5.45	-0.90

PA: Peak area

Chapter IV

Tumor necrosis factor – alpha

4.1. Cytokines - introduction

Cytokines are small proteinaceous signaling molecules, usually less than 80 K Da in size [137,138]. They are produced by all nucleated cells and function as messengers or local hormones, regulating a wide range of biological functions such as inflammation and repair, innate and acquired immunity, hematopoiesis. In the case of inflammation, their action is pleiotropic in nature, that is they play a key role not only in the initiation and perpetuation but also the down regulation of the inflammation process [139,140]. Cytokines are produced in response to both immune and non-immune events. If they are produced as a response to an immune reaction, they are produced in the effector phase of the immune response and control the immune and inflammatory responses [141]. Cytokines are divided into many types, including the hematopoietic family (interleukins), the interferon family (IFN- α , β , γ), the chemokine family, the tumor necrosis family, colony stimulating factors (GM-CSF, G-CSF, M-CSF), and stem cell factors. These play a vital role in many physiological processes [140,141]. Current research project would focus on

proinflammatory cytokines such as IL-1 β , IL-6, TNF- α and chemokine CCL-2. The current chapter would mainly focus on TNF- α . Cytokines are very potent and are present in extremely low concentrations in the body. The concentration ranges from 1 pg/mL – 10 pg/mL [142,143]

4.1.1. Tumor necrosis factor – alpha (TNF- α):

Tumor necrosis factor alpha (TNF- α) is a pro-inflammatory cytokine which is pleiotropic in nature. It has a variety of functions including an influence on sleep, regulation of immune response and immune system homeostasis, apoptosis, cell proliferation and differentiation [144–146]. It is also important for resistance to infection and cancers. Human TNF- α exists in two forms; a type II transmembrane protein, and a mature soluble protein. The TNF- α transmembrane protein is proteolytically cleaved to yield a soluble, biologically active 157 amino acid protein (17.4 KDa) protein. This protein binds as a trimer to cell membrane receptors (TNFR-1 and TNFR-2) to exerts many of its effects by binding [147].

Amino acid sequence of TNF - α :

VRSSSRTPSDKPVAVHVVANPQAEGQLQWLNRRANALLANGVELRDNQLVVPSE
GLYLIYSQVLFKGGQCPSTHVLLTHTISRIVSYQTKVNLLSAIKSPCQRETPEGA
EAKPWYEPIYLGGVFQLEKGDRLSAEINRPDYLDFAESGQVYFGIIAL [148].

4.2 LC-MS method development

4.2.1 Chemicals

Recombinant human TNF - α standards were purchased from PeproTech (Rocky Hill, NJ). Modified sequence grade trypsin was purchased from Promega corporation (Madison, WI), Ammonium bicarbonate (99% analytical grade) from Sigma (Milwaukee, Wisconsin). LCMS grade acetonitrile was purchased from Fisher scientific (Hampton, NH). Deionized water was obtained from a nanopore diamond water purification system from Thermo Scientific.

4.2.2 Instrumentation

A Shimadzu Nexera UHPLC system with two binary LC-30 AD pumps, a DUG20A3R degasser, SIL-30 AC autosampler, CTO-10AVP column oven and a CBM 20A controller interfaced with an AB SCIEX 5500 QTRAP mass spectrometer with Electro Spray Ionization probe and a syringe pump has been used for the purpose of quantification. Instrument operation, acquisition and processing data was performed using AB SCIEX Analyst software.

4.2.3 Liquid chromatography

A reversed phase chromatographic column was considered for the analysis of TNF - α . A linear gradient technique at 30⁰C going from 2% mobile phase B to 40% B in 1 minute and 40% to 90% in 10 minutes was utilized for the elution of the digested protein. Halo Peptide 2 ES-C18 column (Advanced Material Technology, Chadds Ford, PA, USA) (50 x 2.1 mm, 2 μ m) with 0.1% formic acid in water as mobile phase A and 0.1% formic acid in acetonitrile as mobile phase B, pumped at a flow rate of 0.200 mL/min. Post run

column wash and equilibration has been incorporated in the gradient program. For each analysis, 10.0 μL of sample was injected into the system by autosampler set at 10°C, and the gradient time was 20 minutes. A 10-minute equilibration cycles were also included within the gradient.

4.2.4 Tandem mass spectrometry

The compound and source dependent parameters were optimized for the best signal intensity and the conditions were as follows: curtain gas: 40 psi; ion spray voltage: 4000 V; ion spray temperature: 400°C; ion source gas 1: 30 psi; ion source gas 2: 20; declustering potential: 40 V; entrance potential: 10 V; collision energy: 30 eV and cell exit potential: 15 eV.

4.2.5 Preparation of stock and working standard solutions

Stock solution of the protein was prepared by reconstituting the solid TNF - α standard at room temperature with deionized water to make a 1 mg/mL solution. The stock solution was aliquoted into 50 protein low bind tubes and stored at -80°C. One of the aliquots was diluted to 0.1 mg/mL using ammonium bicarbonate solution at pH 7.8. Dilute 20 μL of TNF WS with 30 μL of 2 % ACN and add 100 μL of ACN with 2 % FA. Shake the solution for 5 minutes and centrifuge at 1500 rpm for 1 minute and 2000 rpm for 2 minutes at 4°C. Collect the supernatant and add 10 μL of 0.1 % BSA to it. The sample is then dried under Nitrogen at 30°C. The dried sample is reconstituted with 100 μL of digestion buffer (50 mM ammonium bicarbonate in 10% acetonitrile in water. The solution is mixed well, and trypsin was added to the solution (protease: protein 1:20). This solution is Incubated at 37°C for 12 hours. After the incubation, the solution was cooled down to room temperature and 3 μL of 80 % formic acid was added to quench the digestion process.

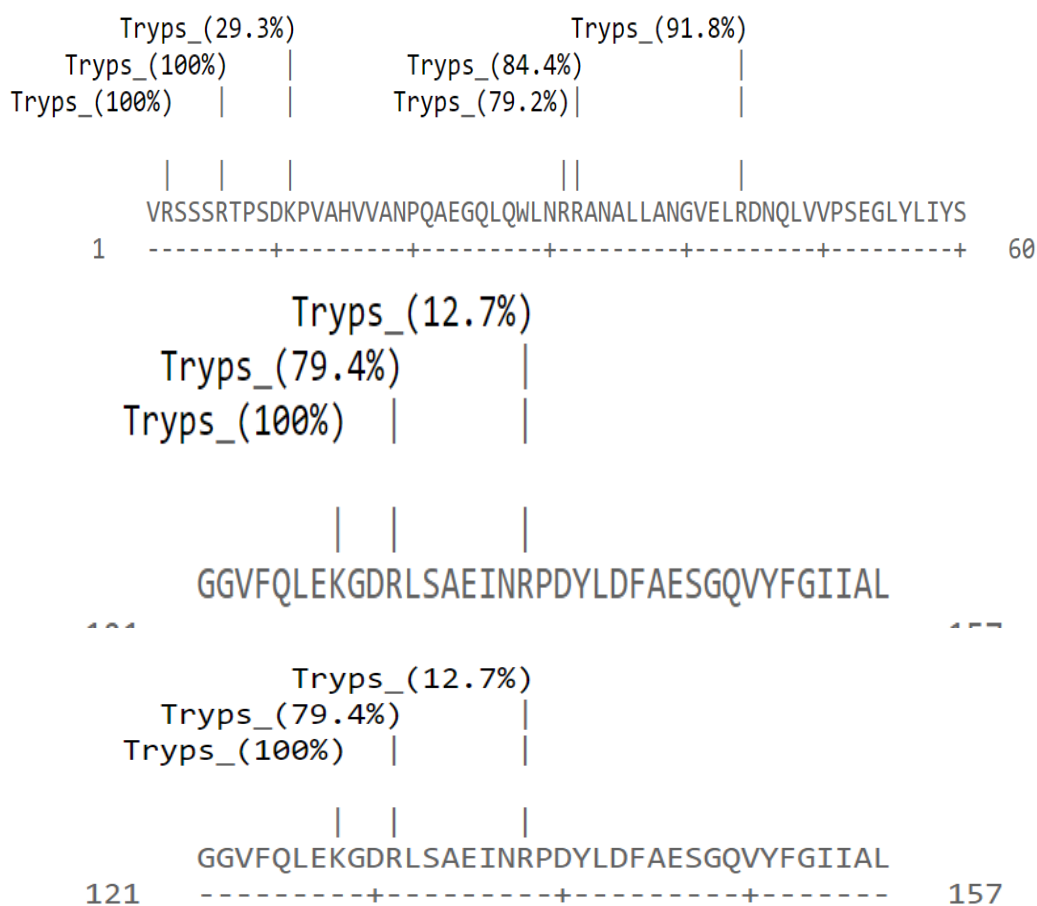
This solution is mixed well for 10 seconds. The solution is centrifuged for 30 seconds to remove any small particulate matter that might be suspended in the solution. The digested protein solution was diluted using 0.1% formic acid and 2 % acetonitrile in deionized water for positive mode and 0.05% ammonium hydroxide and 2 % acetonitrile in deionized water for negative mode mass spectrometry analysis.

4.2.6 Preliminary in-silico experiments:

a. In-silico digestion:

Initial digestion experiments were performed on online proteomics tools such as ExPASy : SIB Bioinformatics Resource Portal using the sophisticated algorithm for trypsin digestion [149] which gives the probability of digestion at all the cleavage sites as a percent value as shown in Figure 32.

Figure 31: In-silico digested protein showing cleavage sites and probability



b. Calculations of theoretical fragmentation pattern

Theoretical fragmentation is important for the optimization of mass spectrometry parameters. The m/z can be theoretically calculated based on the number of acidic and basic amino acids in the protein and the mode being used in the mass spectrometry analysis. The calculated m/z 's are shown in XXXII, Molecular weight of fragments accounting for alkylation during sample preparation as shown in Table XXXIII. m/z of the Theoretical fragments in positive mode and negative modes are shown in Table XXXIV and Table XXXV respectively.

Table XXXII: Theoretical or calculated molecular weights

Resulting peptide sequence	Number of Cysteines	Weight to be added	Final MW
PVAHVVANPQAEGQLQWLNR	-	-	2227.511
ANALLANGVELR	-	-	1240.425
DNQLVVPSEGLYLIYSQVLFK	-	-	2425.807
GQGCPSTHVLLTHTISR	1	57	1,864.057
PWYEPIYLGGVFQLEK	-	-	1939.241
PDYLDFAESGQVYFGIHAL	-	-	2118.370

Table XXXIII: Molecular weight of fragments accounting for alkylation during sample preparation

Position of cleavage site	Name of cleaving enzyme(s)	Resulting peptide sequence (see <u>explanations</u>)	Peptide length [aa]	Peptide mass [Da]	Cleavage probability
31	Trypsin	PVAHVVANPQAEGQLQWLNR	20	2227.511	79.2 %
44	Trypsin	ANALLANGVELR	12	1240.425	91.8 %
65	Trypsin	DNQLVVPSEGLYLIYSQVLFK	21	2425.807	100 %
82	Trypsin	GQGCPSTHVLLTHTISR	17	1807.057	100 %
128	Trypsin	PWYEPIYLGGVFQLEK	16	1939.241	100 %
157	end of sequence	PDYLDFAESGQVYFGIHAL	19	2118.370	-

Table XXXIV: m/z of the Theoretical fragments in positive mode

Resulting peptide sequence	Cleavage probability	Number of + charges	Final MW	m/z
PVAHVVANPQAEGQLQWLNR	79.2 %	2	2227.5	1,114.7, 2228.5
ANALLANGVELR	91.8 %	1	1240.4	1241.4
DNQLVVPSEGLYLIYSQVLFK	100 %	1	2425.8	2426.8
GQGCPSTHVLLTHTISR	100 %	3	1,864.1	622.3 (+3), 933.0 (+2), 1865.1 (+1)
PWYEPIYLGGVFQLEK	100 %	1	1939.2	1940.2
PDYLDFAESGQVYFGIHAL	-	0	2118.4	-

Table XXXV: m/z of the Theoretical fragments in negative mode

Resulting peptide sequence	Cleavage probability	Number of - charges	Final MW	m/z
PVAHVVANPQAEGQLQWLNR	79.2 %	1	2227.5	2226.5
ANALLANGVELR	91.8 %	1	1240.4	1239.4
DNQLVVPSEGLYLIYSQVLFK	100 %	2	2425.8	1211.9 (-2), 2424.8 (-1)
GQGCPSTHVLLTHTISR	100 %	0	1,864.1	-
PWYEPIYLGGVFQLEK	100 %	2	1939.2	968.6
PDYLDFAESGQVYFGIHAL	-	3	2118.4	705.13 (-3), 1058.2 (-2), 2117.4 (-1)

Recombinant TNF alpha Human	
	R.TPSDKPVAHVWANPQAEGQLQWLNR.R [6, 30]
	R.RANALLANGVELR.D [31, 43] (missed 1)
	R.ANALLANGVELR.D [32, 43]
	R.DNQLWVPSEGLYLIYSQVLFK.G [44, 64]
	R.IAVSYQTK.V [82, 89]
	R.IAVSYQTKVNLLSAIK.S [82, 97] (missed 1)
	K.VNLLSAIK.S [90, 97]
	R.ETPEGAEAKPWYEPIYLGGVFQLEK.G [103, 127]

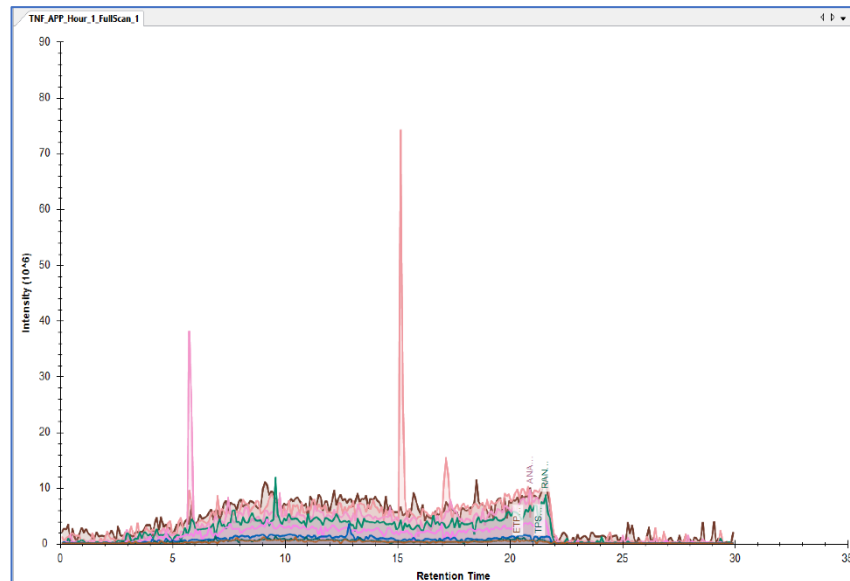


Figure 32 : Deconvoluted chromatogram showing the peak for one of the digested peptides of TNF- α (pink colored peak)

4.2.7 Mass spectrometry analysis

A full scan analysis of TNF – α was performed both in positive and negative mode to confirm the presence the molecule and to optimize the mass spectrometer parameters. The data from the initial experiments was deconvoluted using an online bioinformatics software called SKYLINE. The deconvoluted data showed a large peak for one of the peptides and seven other peptides detected shown in Figure 33 and the expected sequences of the peak is shown in Figure 34

4.3 Future experiments

4.3.1 Sample preparation

- a. Sample clean up and separation of the protein from other proteins: The peptide fragments that had very low intensity causing them to be below the threshold of detection during the initial analysis can be detected by optimizing the sample preparation and reducing the background interference. This can be done by multiple ways. A few methods that can be effective are [150]
 1. Spin filters MWCO 15 KDa
 2. SPE
 3. Immunopeptide capture
 4. Immunochemistry-based liquid chromatographic separations
 5. Capillary electrophoresis/immunochemistry-based separations
 6. Antibody flow-based assays
- b. Optimizing digestion efficiency: Bottom-up proteomics relies on the generated fragments after digestion for detecting the protein. Improving/optimizing the digestion efficiency will improve the sensitivity of the assay as it will generate the maximum

possible fragments without the loss of protein. This can be done by multiple experiments such as

1. Analyzing protein at varying temperatures and duration of digestion to determine the optimal combination of the two parameters.
2. Digesting protein at different trypsin to protein ratio to find the optimal combination.

4.3.2 LC-MS optimization

- a. Optimizing the full scan analysis parameters
- b. Generating an MS/MS fragmentation pattern for all the peptides that can be detected and optimizing the MRM parameters for the peptides.

Optimize the method for biological matrices such as serum and cerebro spinal fluid.

CHAPTER V

FUTURE DIRECTIONS

Current work has chromatographically separated dynorphin A, Dynorphin B and alpha neoendorphin successfully. An LC-MS/MS method has been developed and validated to quantify the standards of dynorphin A, dynorphin B and alpha-neoendorphin spiked in serum at the low physiological concentrations for dynorphin A and dynorphin B. This method will be used to analyze and quantify the basal levels of dynorphin A, dynorphin B and alpha-neoendorphin in a mouse. The method will be further cross validated in CSF to increase the utility of the method to multiple matrices.

Preliminary work on LC-MS/MS analysis of TNF α has been done and was able to detect the standards. This method will be optimized and validated in serum and CSF. The scope for future work will include a complete LC-MS/MS method development and validation of cytokines TNF α , IL-1 α , IL-6 and the chemokine MCP-1/CCL2 in human serum, which will be cross validated in CSF. Method will be validated for accuracy, precision,

limit of detection, lower limit of quantification, stability, extraction recovery and matrix effect following the FDA guidelines for bioanalytical method validation.

Eventually, chromatography will be optimized to resolve dynorphin A, dynorphin B, alpha-neoendorphin, TNF α , IL-1 α , IL-6 and MCP-1/CCL2 using a single method, improving the throughput and efficiency for sample analysis. This method will be used to do a time study in artificially stressed animal models which will establish the effect of dynorphins on major proinflammatory cytokines and chemokines and thus the process of inflammation.

REFERENCES

- [1] J.E. Pascoe, K.L. Williams, P. Mukhopadhyay, K.C. Rice, J.H. Woods, M.C. Ko, Effects of mu, kappa, and delta opioid receptor agonists on the function of hypothalamic-pituitary-adrenal axis in monkeys, *Psychoneuroendocrinology*. 33 (2008) 478–486. doi:10.1016/j.psyneuen.2008.01.006.
- [2] C. Schwarzer, 30 years of dynorphins - New insights on their functions in neuropsychiatric diseases, *Pharmacol. Ther.* 123 (2009) 353–370. doi:10.1016/j.pharmthera.2009.05.006.
- [3] W. Wittmann, E. Schunk, I. Rosskothén, S. Gaburro, N. Singewald, H. Herzog, C. Schwarzer, Prodynorphin-derived peptides are critical modulators of anxiety and regulate neurochemistry and corticosterone, *Neuropsychopharmacology*. 34 (2009) 775–785. doi:10.1038/npp.2008.142.
- [4] E. Bivehed, R. Strömvall, J. Bergquist, G. Bakalkin, M. Andersson, Region-specific bioconversion of dynorphin neuropeptide detected by in situ histochemistry and MALDI imaging mass spectrometry, *Peptides*. 87 (2017) 20–27. doi:10.1016/j.peptides.2016.11.006.
- [5] A. Minokadeh, L. Funkelstein, T. Toneff, S.R. Hwang, M. Beinfeld, T. Reinheckel, C. Peters, J. Zadina, V. Hook, Cathepsin L participates in dynorphin production in brain cortex, illustrated by protease gene knockout and expression, *Mol. Cell. Neurosci.* 43 (2010) 98–107. doi:10.1016/j.mcn.2009.10.001.

- [6] H. Khachaturian, S.J. Watson, M.E. Lewis, D. Coy, A. Goldstein, H. Akil, Dynorphin immunocytochemistry in the rat central nervous system, *Peptides*. 3 (1982) 941–954. doi:10.1016/0196-9781(82)90063-8.
- [7] D. Maysinger, V. Höllt, B.R. Seizinger, P. Mehraein, A. Pasi, A. Herz, Parallel distribution of immunoreactive α -neo-endorphin and dynorphin in rat and human tissue, *Neuropeptides*. 2 (1982) 211–225. doi:10.1016/0143-4179(82)90054-3.
- [8] S.R. Vincent, T. Hökfelt, I. Christensson, L. Terenius, Dynorphin-immunoreactive neurons in the central nervous system of the rat, *Neurosci. Lett.* 33 (1982) 185–190. doi:10.1016/0304-3940(82)90249-X.
- [9] S.J. Watson, H. Khachaturian, L. Taylor, W. Fischlit, A. Goldstein, H. Akil, Pro-dynorphin peptides are found in the same neurons throughout rat brain: Immunocytochemical study (dynorphin/ α -neo-endorphin/neuropeptide/neuroanatomy), 1983.
- [10] C.R. Neal, S.W. Newman, Prodynorphin Peptide Distribution in the Forebrain of the Syrian Hamster and Rat: A Comparative Study With Antisera Against Dynorphin A, Dynorphin B, and the C-Terminus of the Prodynorphin Precursor Molecule, 1989.
- [11] O. Civelli, J. Douglass, A. Goldstein, E. Herbert, Sequence and expression of the rat prodynorphin gene, *Proc. Natl. Acad. Sci. U. S. A.* 82 (1985) 4291–4295. doi:10.1073/pnas.82.12.4291.

- [12] I. Nylander, K. Tan-No, A. Winter, J. Silberring, Processing of prodynorphin-derived peptides in striatal extracts. Identification by electrospray ionization mass spectrometry linked to size-exclusion chromatography, *Life Sci.* 57 (1995) 123–129. doi:10.1016/0024-3205(95)00253-3.
- [13] J.K. Zubieta, Forebrain Opiates, in: *Senses A Compr. Ref.*, Elsevier Inc., 2008: pp. 821–831. doi:10.1016/B978-012370880-9.00199-7.
- [14] E. Weber, C.J. Evans, J.K. Chang, J.D. Barchas, Brain distributions of α -neo-endorphin and β -neo-endorphin: Evidence for regional processing differences, *Biochem. Biophys. Res. Commun.* 108 (1982) 81–88. doi:10.1016/0006-291X(82)91834-4.
- [15] C. Chavkin, Dynorphin-Still an Extraordinarily Potent Opioid Peptide, *Mol. Pharmacol. Mol Pharmacol.* 83 (2013) 729–736. doi:10.1124/mol.112.083337.
- [16] R. Quirion, Pain, nociception and spinal opioid receptors, *Prog. Neuropsychopharmacol. Biol. Psychiatry.* 8 (1984) 571–579. doi:10.1016/0278-5846(84)90017-4.
- [17] F. Nyberg, I. Christensson-Nylander, L. Terenius, Measurement of Opioid Peptides in Biologic Fluids by Radioimmunoassay, in: Springer, Berlin, Heidelberg, 1987: pp. 227–253. doi:10.1007/978-3-642-71809-0_10.
- [18] A.A. Gutstein HB, Opioid analgesics. In: Goodman and Gilman's *The Pharmacological Basis of Therapeutics* (11th ed.), 2006.

- [19] W.M. Yaksh TL, The Pharmacological Basis of Therapeutics, in: K.B. Brunton LL, Chabner BA (Ed.), *Pharmacol. Basis Ther.*, 12th ed., McGraw-Hill, New York, 2011: pp. 481–525.
- [20] A. Goldstein, W. Fischli, L.I. Lowney, M. Hunkapiller, L. Hood, Porcine pituitary dynorphin: complete amino acid sequence of the biologically active heptadecapeptide., *Proc. Natl. Acad. Sci. U. S. A.* 78 (1981) 7219–7223. doi:10.1073/pnas.78.11.7219.
- [21] S.M. Hall, Y.S. Lee, V.J. Hruby, Dynorphin A analogs for the treatment of chronic neuropathic pain, *Future Med. Chem.* 8 (2016) 165–177. doi:10.4155/fmc.15.164.
- [22] S. V. Gein, Dynorphins in regulation of immune system functions, *Biochem.* 79 (2014) 397–405. doi:10.1134/S0006297914050034.
- [23] B.M. Sharp, S. Roy, J.M. Bidlack, Evidence for opioid receptors on cells involved in host defense and the immune system, *J. Neuroimmunol.* 83 (1998) 45–56. doi:10.1016/S0165-5728(97)00220-8.
- [24] R.M. Ransohoff, A.E. Cardona, The myeloid cells of the central nervous system parenchyma, (n.d.). doi:10.1038/nature09615.
- [25] C.C. Chao, G. Gekker, S. Hu, W.S. Sheng, K.B. Shark, D.F. Bu, S. Archer, J.M. Bidlack, P.K. Peterson, κ opioid receptors in human microglia downregulate human immunodeficiency virus 1 expression, *Proc. Natl. Acad. Sci. U. S. A.* 93 (1996) 8051–8056. doi:10.1073/pnas.93.15.8051.

- [26] L.F. Chuang, T.K. Chuang, K.F. Killam, Q. Qui, X.R. Wang, J.J. Lin, H.F. Kung, W. Sheng, C. Chao, L. Yu, R.Y. Chuang, Expression of kappa opioid receptors in human and monkey lymphocytes, *Biochem. Biophys. Res. Commun.* 209 (1995) 1003–1010. doi:10.1006/bbrc.1995.1597.
- [27] D.M.P. Lawrence, W. El-Hamoulyt, S. Archert, J.F. Learyt, J.M. Bidlack, Identification of κ opioid receptors in the immune system by indirect immunofluorescence (fluorescein/phycoerythrin/arylacetamide/thymocyte), 1995.
- [28] X. Liang, R. Liu, C. Chen, F. Ji, T. Li, Opioid System Modulates the Immune Function: A Review, n.d.
- [29] J.M. Bidlack, Detection and Function of Opioid Receptors on Cells from the Immune System, 2000.
- [30] K. Hagi, K. Uno, K. Inaba, S. Muramatsu, Augmenting effect of opioid peptides on murine macrophage activation, *J. Neuroimmunol.* 50 (1994) 71–76. doi:10.1016/0165-5728(94)90216-X.
- [31] M.R. Ruff, S.M. Wahl, S. Mergenhagen, C.B. Pert, Opiate receptor-mediated chemotaxis of human monocytes, *Neuropeptides.* 5 (1985) 363–366. doi:10.1016/0143-4179(85)90029-0.
- [32] C.C. Chao, G. Gekker, S. Hu, W.S. Sheng, P.S. Portoghese, P.K. Peterson, Upregulation of HIV-1 expression in cocultures of chronically infected promonocytes and human brain cells by dynorphin, *Biochem. Pharmacol.* 50 (1995) 715–722. doi:10.1016/0006-2952(95)00176-Z.

- [33] B.M. Sharp, W.F. Keane, H.J. Suh, G. Gekker, D. Tsukayama, P.K. Peterson, OPIOID PEPTIDES RAPIDLY STIMULATE SUPEROXIDE PRODUCTION BY HUMAN POLYMORPHONUCLEAR LEUKOCYTES AND MACROPHAGES, *Endocrinology*. 117 (1985) 793–795. doi:10.1210/endo-117-2-793.
- [34] R.L. Davis, D.J. Buck, N. Saffarian, C.W. Stevens, The opioid antagonist, β -funaltrexamine, inhibits chemokine expression in human astroglial cells, *J. Neuroimmunol*. 186 (2007) 141–149. doi:10.1016/j.jneuroim.2007.03.021.
- [35] L. Zhang, T.J. Rogers, κ -Opioid Regulation of Thymocyte IL-7 Receptor and C-C Chemokine Receptor 2 Expression, *J. Immunol*. 164 (2000) 5088–5093. doi:10.4049/jimmunol.164.10.5088.
- [36] T. Laughlin, J. Bethea, R. Yezierski, G. Wilcox, Cytokine involvement in dynorphin-induced allodynia, *Pain*. 84 (2000) 159–167. doi:10.1016/S0304-3959(99)00195-5.
- [37] V.K. Shukla, S. Lemaire, Central non-opioid physiological and pathophysiological effects of dynorphin A and related peptides., *J. Psychiatry Neurosci*. 17 (1992) 106–119. <https://www.ncbi.nlm.nih.gov/pmc/articles/PMC1188423/>.
- [38] K.F. Shen, S.M. Crain, Dynorphin prolongs the action potential of mouse sensory ganglion neurons by decreasing a potassium conductance whereas another specific kappa opioid does so by increasing a calcium conductance., *Neuropharmacology*. 29 (1990) 343–9. <http://www.ncbi.nlm.nih.gov/pubmed/1971431> (accessed March 28, 2020).

- [39] L. Chen, L.Y. Huang, Protein kinase C reduces Mg²⁺ block of NMDA-receptor channels as a mechanism of modulation, *Nature*. 356 (1992) 521–523. doi:10.1038/356521a0.
- [40] R. Llinás, J.A. Gruner, M. Sugimori, T.L. McGuinness, P. Greengard, Regulation by synapsin I and Ca(2+)-calmodulin-dependent protein kinase II of the transmitter release in squid giant synapse., *J. Physiol.* 436 (1991) 257–282. doi:10.1113/jphysiol.1991.sp018549.
- [41] R.A. Nichols, T.S. Sihra, A.J. Czernik, A.C. Nairn, P. Greengard, Calcium/calmodulin-dependent protein kinase II increases glutamate and noradrenaline release from synaptosomes, *Nature*. 343 (1990) 647–651. doi:10.1038/343647a0.
- [42] A.I. Faden, Opioid and nonopioid mechanisms may contribute to dynorphin's pathophysiological actions in spinal cord injury, *Ann. Neurol.* 27 (1990) 67–74. doi:10.1002/ana.410270111.
- [43] S.R. Kelso, T.E. Nelson, J.P. Leonard, Protein kinase C-mediated enhancement of NMDA currents by metabotropic glutamate receptors in *Xenopus* oocytes., *J. Physiol.* 449 (1992) 705–718. doi:10.1113/jphysiol.1992.sp019110.
- [44] R.M. Caudle, R. Dubner, Ifenprodil blocks the excitatory effects of the opioid peptide dynorphin 1–17 on NMDA receptor-mediated currents in the CA3 region of the guinea pig hippocampus, *Neuropeptides*. 32 (1998) 87–95. doi:10.1016/S0143-4179(98)90022-1.

- [45] L. Guerrini, F. Blasi, S. Denis-Donini, Synaptic activation of NF- κ B by glutamate in cerebellar granule neurons in vitro, 1995.
- [46] C. Kaltschmidt, B. Kaltschmidt, J. Lannes-Vieira, G.W. Kreutzberg, H. Wekerle, P.A. Baeuerle, J. Gehrmann, Transcription factor NF- κ B is activated in microglia during experimental autoimmune encephalomyelitis, *J. Neuroimmunol.* 55 (1994) 99–106. doi:10.1016/0165-5728(94)90151-1.
- [47] T.L. Sahley, D.J. Anderson, M.D. Hammonds, K. Chandu, F.E. Musiek, Evidence for a dynorphin-mediated inner ear immune/inflammatory response and glutamate-induced neural excitotoxicity: An updated analysis, *J. Neurophysiol.* 122 (2019) 1421–1460. doi:10.1152/jn.00595.2018.
- [48] Y.-J. Gao, L. Zhang, R.-R. Ji, Spinal injection of TNF- α -activated astrocytes produces persistent pain symptom mechanical allodynia by releasing monocyte chemoattractant protein-1, *Glia.* 58 (2010) 1871–1880. doi:10.1002/glia.21056.
- [49] Y.J. Gao, L. Zhang, O.A. Samad, M.R. Suter, K. Yasuhiko, Z.Z. Xu, J.Y. Park, A.L. Lind, Q. Ma, R.R. Ji, JNK-induced MCP-1 production in spinal cord astrocytes contributes to central sensitization and neuropathic pain, *J. Neurosci.* 29 (2009) 4096–4108. doi:10.1523/JNEUROSCI.3623-08.2009.
- [50] L. Guan, R. Townsend, T.K. Eisenstein, M.W. Adler, T.J. Rogers, Both T-Cells and Macrophages Are Targets of κ -Opioid-Induced Immunosuppression, *Brain Behav. Immun.* 8 (1994) 229–240. doi:10.1006/brbi.1994.1021.

- [51] J.S. Foster, R.N. Moore, Dynorphin and Related Opioid Peptides Enhance Tumoricidal Activity Mediated by Murine Peritoneal Macrophages, *J. Leukoc. Biol.* 42 (1987) 171–174. doi:10.1002/jlb.42.2.171.
- [52] I.H. Jonsdottir, Neuropeptides and their interaction with exercise and immune function, *Immunol. Cell Biol.* 78 (2000) 562–570. doi:10.1111/j.1440-1711.2000.t01-10-.x.
- [53] J.-S. Han, C.-W. Xie, Dynorphin: Potent analgesic effect in spinal cord of the rat, *Life Sci.* 31 (1982) 1781–1784. doi:10.1016/0024-3205(82)90209-0.
- [54] T. Nakazawa, M. Ikeda, T. Kaneko, K. Yamatsu, Analgesic effects of dynorphin-A and morphine in mice, *Peptides.* 6 (1985) 75–78. doi:10.1016/0196-9781(85)90079-8.
- [55] S. Lyrenäs, F. Nyberg, H. Lutsch, B. Lindberg, L. Terenius, Cerebrospinal fluid dynorphin1-17 and beta-endorphin in late pregnancy and six months after delivery. No influence of acupuncture treatment, *Acta Endocrinol. (Copenh).* 115 (1987) 253–258. <http://www.ncbi.nlm.nih.gov/pubmed/2885996>.
- [56] J. Lai, M.H. Ossipov, T.W. Vanderah, T.P. Malan, F. Porreca, Neuropathic pain: the paradox of dynorphin., *Mol. Interv.* 1 (2001) 160–7. <http://www.ncbi.nlm.nih.gov/pubmed/14993349> (accessed August 19, 2019).
- [57] K.C. Kajander, Y. Sahara, M.J. Iadarola, G.J. Bennett, Dynorphin increases in the dorsal spinal cord in rats with a painful peripheral neuropathy, *Peptides.* 11 (1990) 719–728. doi:10.1016/0196-9781(90)90187-A.

- [58] C.M. Handler, E.B. Geller, M.W. Adler, Effect of μ -, κ -, and δ -selective opioid agonists on thermoregulation in the rat, *Pharmacol. Biochem. Behav.* 43 (1992) 1209–1216. doi:10.1016/0091-3057(92)90504-9.
- [59] A.I. Faden, T.P. Jacobs, Dynorphin-related peptides cause motor dysfunction in the rat through a non-opiate action., *Br. J. Pharmacol.* 81 (1984) 271–276. <https://www.ncbi.nlm.nih.gov/pmc/articles/PMC1986877/>.
- [60] A.I. Faden, C.J. Molineaux, J.G. Rosenberger, T.P. Jacobs, B.M. Cox, Increased dynorphin immunoreactivity in spinal cord after traumatic injury, *Regul. Pept.* 11 (1985) 35–41. doi:10.1016/0167-0115(85)90029-1.
- [61] M.S. Kannan, A.E. Seip, Neurogenic dilatation and constriction of rat superior mesenteric artery in vitro: mechanisms and mediators, *Can. J. Physiol. Pharmacol.* 64 (1986) 729–736. doi:10.1139/y86-123.
- [62] G.G.Z. Feuerstein, A.L. Sirén, The opioid system in cardiac and vascular regulation of normal and hypertensive states., *Circulation.* 75 (1987) NaN-NaN. <https://pdfs.semanticscholar.org/bcc0/049703d5e9bb540026071a11323e211239d2.pdf>.
- [63] Role of endomorphin in the mouse brain: Full Text Search Results, (2019). [http://resolver.ebscohost.com/openurl?sid=CAS%3ACAPLUS&coden=69ART5&genre=article&date=1999&spage=63&epage=67&title=Shokakan+Horumon+\(XVII\)%2C+Gut+Hormone+Kanfaransu+Kirokushu%2C+20th%2C+Japan%2C+1999&stitle=Shokakan+Horumon+\(XVII\)%2C+Gut+Horm.+Kanfaransu](http://resolver.ebscohost.com/openurl?sid=CAS%3ACAPLUS&coden=69ART5&genre=article&date=1999&spage=63&epage=67&title=Shokakan+Horumon+(XVII)%2C+Gut+Hormone+Kanfaransu+Kirokushu%2C+20th%2C+Japan%2C+1999&stitle=Shokakan+Horumon+(XVII)%2C+Gut+Horm.+Kanfaransu).

- [64] A. Inutsuka, A. Inui, S. Tabuchi, T. Tsunematsu, M. Lazarus, A. Yamanaka, Concurrent and robust regulation of feeding behaviors and metabolism by orexin neurons, *Neuropharmacology*. 85 (2014) 451–460. doi:10.1016/j.neuropharm.2014.06.015.
- [65] A.L.O. Hebb, S. Laforest, G. Drolet, Chapter 4.9 - Endogenous opioids, stress, and psychopathology, in: T. Steckler, N.H. Kalin, J.M.H.M. Reul (Eds.), *Tech. Behav. Neural Sci.*, Elsevier, 2005: pp. 561–583. <http://www.sciencedirect.com/science/article/pii/S0921070905800318>.
- [66] K.F. Shen, S.M. Crain, Dynorphin prolongs the action potential of mouse sensory ganglion neurons by decreasing a potassium conductance whereas another specific kappa opioid does so by increasing a calcium conductance, *Neuropharmacology*. 29 (1990) 343–349. <http://www.ncbi.nlm.nih.gov/pubmed/1971431>.
- [67] T.L. Sahley, D.J. Anderson, M.D. Hammonds, K. Chandu, F.E. Musiek, Evidence for a dynorphin-mediated inner ear immune/inflammatory response and glutamate-induced neural excitotoxicity: an updated analysis, *J. Neurophysiol.* 122 (2019) 1421–1460. doi:10.1152/jn.00595.2018.
- [68] Y. Chen, C. Chen, L.Y. Liu-Chen, Dynorphin peptides differentially regulate the human κ opioid receptor, *Life Sci.* 80 (2007) 1439–1448. doi:10.1016/j.lfs.2007.01.018.

- [69] J.-L. Montiel, F. Cornille, B.P. Roques, F. Noble, Nociceptin/Orphanin FQ Metabolism: Role of Aminopeptidase and Endopeptidase 24.15, *J. Neurochem.* 68 (2002) 354–361. doi:10.1046/j.1471-4159.1997.68010354.x.
- [70] B. Reed, J.M. Bidlack, B.T. Chait, M.J. Kreek, Extracellular Biotransformation of β -Endorphin in Rat Striatum and Cerebrospinal Fluid, *J. Neuroendocrinol.* 20 (2008) 606–616. doi:10.1111/j.1365-2826.2008.01705.x.
- [71] J. Sandin, I. Nylander, J. Silberring, Metabolism of β -endorphin in plasma studied by liquid chromatography-electrospray ionization mass spectrometry, *Regul. Pept.* 73 (1998) 67–72. doi:10.1016/S0167-0115(97)01065-3.
- [72] C. Sakurada, S. Sakurada, T. Hayashi, S. Katsuyama, K. Tan-No, T. Sakurada, Degradation of endomorphin-2 at the supraspinal level in mice is initiated by dipeptidyl peptidase IV: An in vitro and in vivo study, *Biochem. Pharmacol.* 66 (2003) 653–661. doi:10.1016/S0006-2952(03)00391-5.
- [73] S. Müller, G. Hochhaus, Metabolism of Dynorphin A 1-13 in Human Blood and Plasma, *Pharm. Res. An Off. J. Am. Assoc. Pharm. Sci.* 12 (1995) 1165–1170. doi:10.1023/A:1016211910107.
- [74] A.M.B.H.L.C.G. Safavi, Purification and characterization of a secreted T cell β -endorphin endopeptidase, *Adv. Exp. Med. Biol.* 402 (1996) 71–79.
- [75] M. Morgan, H.M.D.R. Herath, P.J. Cabot, P.N. Shaw, A.K. Hewavitharana, Dynorphin A 1-17 biotransformation in inflamed tissue, serum and trypsin solution analysed by liquid chromatography-tandem mass spectrometry, *Anal. Bioanal.*

Chem. 404 (2012) 3111–3121. doi:10.1007/s00216-012-6406-8.

- [76] I. Lantz, L. Terenius, High enkephalyl peptide degradation, due to angiotensin-converting enzyme-like activity in human CSF, *FEBS Lett.* 193 (1985) 31–34. doi:10.1016/0014-5793(85)80073-9.
- [77] B. Reed, Y. Zhang, B.T. Chait, M.J. Kreek, Dynorphin A(1-17) biotransformation in striatum of freely moving rats using microdialysis and matrix-assisted laser desorption/ionization mass spectrometry, *J. Neurochem.* 86 (2003) 815–823. doi:10.1046/j.1471-4159.2003.01859.x.
- [78] J.Z. Chou, B.T. Chait, R. Wang, M.J. Kreek, Differential biotransformation of dynorphin A(1-17) and dynorphin A(1-13) peptides in human blood, *ex vivo*, *Peptides.* 17 (1996) 983–990. doi:10.1016/0196-9781(96)00154-4.
- [79] Q. Li, J.-K. Zubieta, R.T. Kennedy, Practical Aspects of *in Vivo* Detection of Neuropeptides by Microdialysis Coupled Off-Line to Capillary LC with Multistage MS, *Anal. Chem.* 81 (2009) 2242–2250. doi:10.1021/ac802391b.
- [80] C.D.K. Sloan, *The Development of Analytical Methods for Investigations of Dynorphin A 1-17 Metabolism in the Central Nervous System and Peripheral Tissues and Transport at the Blood Brain Barrier*, University of Kansas, 2005.
- [81] E. Bertol, F. Vaiano, M. Borsotti, M. Quercioli, F. Mari, Comparison of immunoassay screening tests and LC-MS-MS for urine detection of benzodiazepines and their metabolites: results of a national proficiency test., *J. Anal. Toxicol.* 37 (n.d.) 659–64. doi:10.1093/jat/bkt063.

- [82] K. Yücel, S. Abuşoğlu, A. Ünlü, Comparison of immunoassay and liquid chromatography-tandem mass spectrometry methods in the measurement of serum androstenedione levels, *Clin. Lab.* 64 (2018) 69–75. doi:10.7754/Clin.Lab.2017.170612.
- [83] L. Prokai, H.-S. Kim, A. Zharikova, J. Roboz, L. Ma, L. Deng, W.J. Simonsick, Electrospray ionization mass spectrometric and liquid chromatographic–mass spectrometric studies on the metabolism of synthetic dynorphin A peptides in brain tissue in vitro and in vivo, *J. Chromatogr. A.* 800 (1998) 59–68. doi:10.1016/S0021-9673(97)01295-8.
- [84] A. Ljungdahl, J. Hanrieder, M. Fälth, J. Bergquist, M. Andersson, Imaging Mass Spectrometry Reveals Elevated Nigral Levels of Dynorphin Neuropeptides in L-DOPA-Induced Dyskinesia in Rat Model of Parkinson’s Disease, *PLoS One.* 6 (2011). doi:10.1371/journal.pone.0025653.
- [85] J. Hanrieder, A. Ljungdahl, M. Fälth, S.E. Mammo, J. Bergquist, M. Andersson, L-DOPA-induced Dyskinesia is Associated with Regional Increase of Striatal Dynorphin Peptides as Elucidated by Imaging Mass Spectrometry, *Mol. Cell. Proteomics.* 10 (2011). doi:10.1074/mcp.M111.009308.
- [86] J. Hanrieder, A. Ljungdahl, M. Andersson, MALDI Imaging Mass Spectrometry of Neuropeptides in Parkinson’s Disease, *J. Vis. Exp.* (2012). doi:10.3791/3445.
- [87] F. Beaudry, C.E. Ferland, P. Vachon, Identification, characterization and quantification of specific neuropeptides in rat spinal cord by liquid chromatography

- electrospray quadrupole ion trap mass spectrometry, *Biomed. Chromatogr.* 23 (2009) 940–950. doi:10.1002/bmc.1206.
- [88] N.C. Van De Merbel, Protein quantification by LC – MS : a decade of progress through the pages of *Bioanalysis*, 11 (2019) 629–644.
- [89] S.B. Breitkopf, S.J.H. Ricoult, M. Yuan, Y. Xu, D.A. Peake, B.D. Manning, J.M. Asara, A relative quantitative positive/negative ion switching method for untargeted lipidomics via high resolution LC-MS/MS from any biological source, *Metabolomics*. 13 (2017). doi:10.1007/s11306-016-1157-8.
- [90] S. Eliuk, A. Makarov, *Evolution of Orbitrap Mass Spectrometry Instrumentation*, (2015). doi:10.1146/annurev-anchem-071114-040325.
- [91] M. Ghaste, R. Mistrik, V. Shulaev, Applications of fourier transform ion cyclotron resonance (FT-ICR) and orbitrap based high resolution mass spectrometry in metabolomics and lipidomics, *Int. J. Mol. Sci.* 17 (2016). doi:10.3390/ijms17060816.
- [92] Pros and Cons of Three High-Resolution Mass Spec Approaches | Biocompare: The Buyer's Guide for Life Scientists, (n.d.). <https://www.biocompare.com/Editorial-Articles/338099-Pros-and-Cons-of-Three-High-Resolution-Mass-Spec-Approaches/> (accessed February 7, 2020).
- [93] (No Title), (n.d.). <http://web.gps.caltech.edu/~als/IRMS/course-materials/lecture-6--mass-analyzers/lecture-6-notes.pdf> (accessed February 7, 2020).

- [94] A.D. Catherman, O.S. Skinner, N.L. Kelleher, Top Down Proteomics: Facts and Perspectives, (2014). doi:10.1016/j.bbrc.2014.02.041.
- [95] L.M. Smith, N.L. Kelleher, : N-Kelleher@northwestern Edu, Proteoform: a single term describing protein complexity The Consortium for Top Down Proteomics NIH Public Access, Nat Methods. 10 (2013) 186–187. doi:10.1038/nmeth.2369.
- [96] P.B. Pandeswari, V. Sabareesh, Middle-down approach: a choice to sequence and characterize proteins/proteomes by mass spectrometry †, (2019). doi:10.1039/c8ra07200k.
- [97] T. Wehr, Top-Down versus Bottom-Up Approaches in Proteomics, (n.d.).
- [98] L. Yuan, M. Zhu, Quantitative Bioanalysis of Proteins by Mass Spectrometry, Mater. Methods. 5 (2015) 1–10. doi:10.13070/mm.en.5.1332.
- [99] 5 Insights: Protein Quantification Using the Surrogate Peptide Method - Waters, (n.d.). <https://blog.waters.com/5-insights-regarding-protein-quantification-using-the-surrogate-peptide-method> (accessed April 13, 2020).
- [100] C. López-Otín, L.M. Matrisian, Emerging roles of proteases in tumour suppression, Nat. Rev. Cancer. 7 (2007) 800–808. doi:10.1038/nrc2228.
- [101] Proteolytic enzyme | enzyme | Britannica, (n.d.). <https://www.britannica.com/science/proteolytic-enzyme> (accessed March 9, 2020).
- [102] C. López-Otín, J.S. Bond, Proteases: Multifunctional enzymes in life and disease, J. Biol. Chem. 283 (2008) 30433–30437. doi:10.1074/jbc.R800035200.

- [103] The Mammalian Degradome Database, (n.d.).
<http://degradome.uniovi.es/dindex.html> (accessed March 9, 2020).
- [104] A. Laskar, A. Chatterjee, Protease – Revisiting the Types and potential, *J. Biotechnol.* 1 (2009) 55–61.
- [105] M.B. Rao, A.M. Tanksale, M.S. Ghatge, V. V. Deshpande, Molecular and Biotechnological Aspects of Microbial Proteases †, *Microbiol. Mol. Biol. Rev.* 62 (1998) 597–635. doi:10.1128/membr.62.3.597-635.1998.
- [106] J. Mótyán, F. Tóth, J. Tózsér, Research Applications of Proteolytic Enzymes in Molecular Biology, *Biomolecules.* 3 (2013) 923–942. doi:10.3390/biom3040923.
- [107] S. Unajak, S. Aroonluke, A. Promboon, *Industrial enzyme applications.*, 2015. doi:10.1533/9781782421580.
- [108] L. Tsiatsiani, A.J.R. Heck, Proteomics beyond trypsin, *FEBS J.* 282 (2015) 2612–2626. doi:10.1111/febs.13287.
- [109] S. Heissel, S.J. Frederiksen, J. Bunkenborg Id, P. Højrup Id, Enhanced trypsin on a budget: Stabilization, purification and high-temperature application of inexpensive commercial trypsin for proteomics applications, (n.d.). doi:10.1371/journal.pone.0218374.
- [110] P. Giansanti, L. Tsiatsiani, T.Y. Low, A.J.R. Heck, Six alternative proteases for mass spectrometry-based proteomics beyond trypsin, *Nat. Protoc.* 11 (2016) 993–1006. doi:10.1038/nprot.2016.057.

- [111] D.L. Swaney, C.D. Wenger, J.J. Coon, The value of using multiple proteases for large-scale mass spectrometry-based proteomics, (n.d.). doi:10.1021/pr900863u.
- [112] S. Bischof, J. Grossmann, W. Gruissem, Proteomics and its application in plant biotechnology, in: *Plant Biotechnol. Agric.*, Elsevier Inc., 2012: pp. 55–65. doi:10.1016/B978-0-12-381466-1.00004-3.
- [113] L. Sleno, The use of mass defect in modern mass spectrometry, *J. Mass Spectrom.* 47 (2012) 226–236. doi:10.1002/jms.2953.
- [114] R. Aebersold, M. Mann, Mass spectrometry-based proteomics, *Nature*. 422 (2003) 198–207. doi:10.1038/nature01511.
- [115] O.J. Pozo, P. Van Eenoo, K. Deventer, H. Elbardissy, S. Grimalt, J. V. Sancho, F. Hernandez, R. Ventura, F.T. Delbeke, Comparison between triple quadrupole, time of flight and hybrid quadrupole time of flight analysers coupled to liquid chromatography for the detection of anabolic steroids in doping control analysis, *Anal. Chim. Acta*. 684 (2011) 107–120. doi:10.1016/j.aca.2010.10.045.
- [116] A. Vaghela, A. Patel, A. Patel, A. Vyas, N. Patel, Sample Preparation In Bioanalysis: A Review, *Int. J. Sci. Technol. Res.* 5 (2016) 5. www.ijstr.org (accessed April 18, 2020).
- [117] R. Kong, *Lc/MS application in highthroughput ADME screen*, Elsevier Inc., 2005. doi:10.1016/S0149-6395(05)80061-3.

- [118] S.T. Wu, Z. Ouyang, T. V. Olah, M. Jemal, A strategy for liquid chromatography/tandem mass spectrometry based quantitation of pegylated protein drugs in plasma using plasma protein precipitation with water-miscible organic solvents and subsequent trypsin digestion to generate surrogate peptides for detection, *Rapid Commun. Mass Spectrom.* 25 (2011) 281–290. doi:10.1002/rcm.4856.
- [119] L. Yuan, M. Zhu, Quantitative Bioanalysis of Proteins by Mass Spectrometry, *Mater. Methods.* 5 (2015). doi:10.13070/mm.en.5.1332.
- [120] Z. Ouyang, M.T. Furlong, S. Wu, B. Slecicka, J. Tamura, H. Wang, S. Suchard, A. Suri, T. Olah, A. Tymiak, M. Jemal, Pellet digestion: A simple and efficient sample preparation technique for LC-MS/MS quantification of large therapeutic proteins in plasma, *Bioanalysis.* 4 (2012) 17–28. doi:10.4155/bio.11.286.
- [121] L. Yuan, M.E. Arnold, A.F. Aubry, Q.C. Ji, Simple and efficient digestion of a monoclonal antibody in serum using pellet digestion: Comparison with traditional digestion methods in LC-MS/MS bioanalysis, *Bioanalysis.* 4 (2012) 2887–2896. doi:10.4155/bio.12.284.
- [122] G. Liu, Y. Zhao, A. Angeles, L.L. Hamuro, M.E. Arnold, J.X. Shen, A novel and cost effective method of removing excess albumin from plasma/serum samples and its impacts on LC-MS/MS bioanalysis of therapeutic proteins, *Anal. Chem.* 86 (2014) 8336–8343. doi:10.1021/ac501837t.

- [123] H. Zhang, Q. Xiao, B. Xin, W. Trigona, A.A. Tymiak, A.R. Dongre, T. V. Olah, Development of a highly sensitive liquid chromatography/tandem mass spectrometry method to quantify total and free levels of a target protein, interferon-gamma-inducible protein-10, at picomolar levels in human serum, *Rapid Commun. Mass Spectrom.* 28 (2014) 1535–1543. doi:10.1002/rcm.6928.
- [124] L. Yuan, A.F. Aubry, M.E. Arnold, Q.C. Ji, Systematic investigation of orthogonal SPE sample preparation for the LC-MS/MS bioanalysis of a monoclonal antibody after pellet digestion, *Bioanalysis.* 5 (2013) 2379–2391. doi:10.4155/bio.13.224.
- [125] Z. Yang, M. Hayes, X. Fang, M.P. Daley, S. Effenberg, F.L.S. Tse, LC-MS/MS approach for quantification of therapeutic proteins in plasma using a protein internal standard and 2D-solid-phase extraction cleanup, *Anal. Chem.* 79 (2007) 9294–9301. doi:10.1021/ac0712502.
- [126] Q.C. Ji, R. Rodila, E.M. Gage, T.A. El-Shourbagy, A Strategy of Plasma Protein Quantitation by Selective Reaction Monitoring of an Intact Protein, *Anal. Chem.* 75 (2003) 7008–7014. doi:10.1021/ac034930n.
- [127] Q. Ruan, Q.C. Ji, M.E. Arnold, W.G. Humphreys, M. Zhu, Strategy and its implications of protein bioanalysis utilizing high-resolution mass spectrometric detection of intact protein, *Anal. Chem.* 83 (2011) 8937–8944. doi:10.1021/ac201540t.
- [128] J. Palandra, A. Finelli, M. Zhu, J. Masferrer, H. Neubert, Highly specific and sensitive measurements of human and monkey interleukin 21 using sequential

- protein and tryptic peptide immunoaffinity LC-MS/MS, *Anal. Chem.* 85 (2013) 5522–5529. doi:10.1021/ac4006765.
- [129] N.L. Anderson, N.G. Anderson, L.R. Haines, D.B. Hardie, R.W. Olafson, T.W. Pearson, Mass Spectrometric Quantitation of Peptides and Proteins Using Stable Isotope Standards and Capture by Anti-Peptide Antibodies (SISCAPA), *J. Proteome Res.* 3 (2004) 235–244. doi:10.1021/pr034086h.
- [130] J.R. Whiteaker, L. Zhao, L. Anderson, A.G. Paulovich, An automated and multiplexed method for high throughput peptide immunoaffinity enrichment and multiple reaction monitoring mass spectrometry-based quantification of protein biomarkers, *Mol. Cell. Proteomics.* 9 (2010) 184–196. doi:10.1074/mcp.M900254-MCP200.
- [131] L. Yuan, A. Mai, A.F. Aubry, M.E. Arnold, Q.C. Ji, Feasibility assessment of a novel selective peptide derivatization strategy for sensitivity enhancement for the liquid chromatography/tandem mass spectrometry bioanalysis of protein therapeutics in serum, *Rapid Commun. Mass Spectrom.* 28 (2014) 705–712. doi:10.1002/rcm.6836.
- [132] H. Hahne, F. Pachl, B. Ruprecht, S.K. Maier, S. Klaeger, D. Helm, G. Médard, M. Wilm, S. Lemeer, B. Kuster, DMSO enhances electrospray response, boosting sensitivity of proteomic experiments, *Nat. Methods.* 10 (2013) 989–991. doi:10.1038/nmeth.2610.

- [133] J.G. Meyer, E.A. Komives, Charge state coalescence during electrospray ionization improves peptide identification by tandem mass spectrometry, *J. Am. Soc. Mass Spectrom.* 23 (2012) 1390–1399. doi:10.1007/s13361-012-0404-0.
- [134] P. Feist, A.B. Hummon, Proteomic challenges: Sample preparation techniques for Microgram-Quantity protein analysis from biological samples, *Int. J. Mol. Sci.* 16 (2015) 3537–3563. doi:10.3390/ijms16023537.
- [135] H.J. Issaq, T.P. Conrads, G.M. Janini, T.D. Veenstra, Methods for fractionation, separation and profiling of proteins and peptides, *Electrophoresis.* 23 (2002) 3048–3061. doi:10.1002/1522-2683(200209)23:17<3048::AID-ELPS3048>3.0.CO;2-L.
- [136] W.D. Nes, *Protein Purification: Principles, High-Resolution Methods, and Applications.* Second Edition Edited by Jan-Christer Janson and Lars Rydén (Uppsala University). John Wiley & Sons: New York. 1988. 695 pp. ISBN 0-471-18626-0., *J. Am. Chem. Soc.* 121 (1999) 1625–1625. doi:10.1021/ja985637l.
- [137] K.F. Chung, Cytokines, in: *Asthma COPD*, Elsevier Ltd, 2009: pp. 327–341. doi:10.1016/B978-0-12-374001-4.00027-4.
- [138] V.R. Moulton, Cytokines, in: *Syst. Lupus Erythematosus Basic, Appl. Clin. Asp.*, Elsevier Inc., 2016: pp. 137–141. doi:10.1016/B978-0-12-801917-7.00017-6.
- [139] S. Lata, G.P.S. Raghava, CytoPred: a server for prediction and classification of cytokines., *Protein Eng. Des. Sel.* 21 (2008) 279–82. doi:10.1093/protein/gzn006.

- [140] R. Alam, A brief review of the immune system, *Prim. Care - Clin. Off. Pract.* 25 (1998) 727–738. doi:10.1016/S0095-4543(05)70084-1.
- [141] M.M. Khan, M.M. Khan, Role of Cytokines, in: *Immunopharmacology*, Springer International Publishing, 2016: pp. 57–92. doi:10.1007/978-3-319-30273-7_2.
- [142] R. Kruse, B. Essén-Gustavsson, C. Fossum, M. Jensen-Waern, Blood concentrations of the cytokines IL-1beta, IL-6, IL-10, TNF-alpha and IFN-gamma during experimentally induced swine dysentery, *Acta Vet. Scand.* 50 (2008). doi:10.1186/1751-0147-50-32.
- [143] O. Arican, M. Aral, S. Sasmaz, P. Ciragil, Serum levels of TNF- α , IFN- γ , IL-6, IL-8, IL-12, IL-17, and IL-18 in patients with active psoriasis and correlation with disease severity, *Mediators Inflamm.* 2005 (2005) 273–279. doi:10.1155/MI.2005.273.
- [144] H.Ø. Eggestøl, H.S. Lunde, G.T. Haugland, The proinflammatory cytokines TNF- α and IL-6 in lumpfish (*Cyclopterus lumpus* L.) -identification, molecular characterization, phylogeny and gene expression analyses, *Dev. Comp. Immunol.* 105 (2020) 103608. doi:10.1016/j.dci.2020.103608.
- [145] D.B. Dubravec, D.R. Spriggs, J.A. Mannick, M.L. Rodrick, Circulating human peripheral blood granulocytes synthesize and secrete tumor necrosis factor α , *Proc. Natl. Acad. Sci. U. S. A.* 87 (1990) 6758–6761. doi:10.1073/pnas.87.17.6758.
- [146] J.M. KRUEGER, J. FANG, P. TAISHI, Z. CHEN, T. KUSHIKATA, J. GARDI, Sleep: A Physiologic Role for IL-1beta and TNF-alpha, *Ann. N. Y. Acad. Sci.* 856

(1998) 148–159. doi:10.1111/j.1749-6632.1998.tb08323.x.

[147] H.T. Idriss, J.H. Naismith, TNF α and the TNF receptor superfamily: Structure-function relationship(s), *Microsc. Res. Tech.* 50 (2000) 184–195. doi:10.1002/1097-0029(20000801)50:3<184::AID-JEMT2>3.0.CO;2-H.

[148] Recombinant Human TNF- α , (n.d.). <https://www.peprotech.com/en/recombinant-human-tnf-> (accessed April 29, 2020).

[149] PeptideCutter, (n.d.).
https://web.expasy.org/peptide_cutter/peptidecutter_special_enzymes.html
(accessed April 28, 2020).

[150] J.A. Stenken, A.J. Poschenrieder, Bioanalytical chemistry of cytokines - A review, *Anal. Chim. Acta.* 853 (2015) 95–115. doi:10.1016/j.aca.2014.10.009.